

The influence of shallow-water methane emissions on foraminiferal assemblages: The case of Scoglio d'Affrica (Northern Tyrrhenian Sea, Mediterranean Sea)

Letizia Di Bella^{a,*}, Martina Pierdomenico^b, Aida Maria Conte^b, Irene Cornacchia^b, Tania Ruspandini^a, Daniele Spatola^a, Stanley Eugene Beaubien^a, Sabina Bigi^a, Alessia Conti^b, Giovanni Gaglianone^a, Michela Ingrassia^b, Francesco Latino Chiocci^{a,b}, Daniele Casalbore^{a,b}

^a Department of Earth Sciences, Sapienza University, Piazzale Aldo Moro 5, Rome, Italy

^b Research Council of Italy, Institute of Environmental Geology and Geoengineering (CNR-IGAG), UOS, Department of Earth Sciences, Sapienza University, Piazzale Aldo Moro 5, Rome, Italy

ARTICLE INFO

Keywords:

Benthic foraminifera
Extreme environment
Methane emissions
Mud volcano
Tuscan archipelago

ABSTRACT

Microfaunal analyses were conducted near Scoglio d'Affrica in the Tuscan Archipelago (Northern Tyrrhenian Sea), to study the response of benthic foraminifera to methane (CH₄) venting activity that occurs in this shallow water environment. Our data show that sedimentary processes linked to the CH₄ emissions exert a strong influence on foraminiferal assemblages, resulting in a very patchy spatial distribution linked to complex abiotic and biotic interactions. Methane emissions and mud represent the two main stressor factors for the benthic foraminiferal assemblages, although at present it is not possible to determine which impact dominates.

Five different morphological settings, controlled by venting activity, were defined on and off the mud volcanoes (MVs). Each of these settings has distinct assemblages: 1) areas with strong emission activity at the top of the MVs, locally associated with gryphons and mudflows, where the environmental conditions are clearly prohibitive for foraminiferal life; 2) mud flows along the MV flanks, where overlapping mudflows likely limit foraminiferal colonization; 3) muddy sediments associated with weak emissions where the development of foraminiferal community is favored, although with differences in terms of density, diversity and compositional features linked to the timing of colonization by each species; 4) intermatte zones with scarce or absent emissions, characterized by typical shallow water taxa indicative of well-oxygenated and highly hydrodynamic conditions; and 5) *Posidonia oceanica* substrates, characterized by higher foraminiferal content on the leaves compared to the rhizomes and surrounding sediments; indeed, sediments and rhizomes were more impacted by emissions, whereas *Posidonia* leaves offer "refugia" and a more mitigated environment.

Although it is difficult to define a pattern of biota response and to identify seep-exclusive taxa, foraminifera can represent good environmental proxies for both monitoring the variability of recent venting activity and detecting stressed conditions occurring in the geological record. The seafloor around Scoglio d'Affrica represents a very promising study site for multidisciplinary marine research regarding venting activity, geochemistry of cold seep fluids and their effects on benthic organisms.

1. Introduction

Methane (CH₄) is an important greenhouse gas, with a global warming potential about 20 times larger than carbon dioxide (CO₂) on a

100-year horizon (Ramaswamy et al., 2001). In the marine environment, coastal areas represent methane hotspots, releasing around 8 to 13 Tg CH₄ yr⁻¹ (Bange et al., 1994; Schorn et al., 2022; Rosentreter et al., 2021) and greatly exceeding emissions from the open ocean

* Corresponding author.

E-mail addresses: letizia.dibella@uniroma1.it (L. Di Bella), martina.pierdomenico@cnr.it (M. Pierdomenico), aidamaria.conte@cnr.it (A.M. Conte), irene.cornacchia@igg.cnr.it (I. Cornacchia), tania.ruspandini@uniroma1.it (T. Ruspandini), daniele.spatola@uniroma1.it (D. Spatola), stanley.beaubien@uniroma1.it (S.E. Beaubien), alessia.conti@cnr.it (A. Conti), gaglianone.giovanni@uniroma1.it (G. Gaglianone), michela.ingrassia@cnr.it (M. Ingrassia), francesco.chiocci@uniroma1.it (F.L. Chiocci), daniele.casalbore@uniroma1.it (D. Casalbore).

<https://doi.org/10.1016/j.marpetgeo.2024.107130>

Received 1 May 2024; Received in revised form 19 September 2024; Accepted 23 September 2024

Available online 26 September 2024

0264-8172/© 2024 The Authors. Published by Elsevier Ltd. This is an open access article under the CC BY license (<http://creativecommons.org/licenses/by/4.0/>).

(0.6–1.2 Tg CH₄ yr⁻¹, Rhee et al., 2009). Seafloor areas affected by methane emissions are known as cold seeps, which can be associated with the development of morphologically negative and/or positive structures, such as pockmarks and mud volcanoes (e.g., Hovland et al., 2002; Kopf et al., 2002; Mazzini et al., 2017). Both these structures are the shallow expression of deep fluid migration along fault dislocations and other structural features (Judd and Hovland, 2009). These seafloor areas represent a very peculiar and extreme environment that is considered as a hotspot for most associated benthic assemblages (e.g., Ingrassia et al., 2015; Di Bella et al., 2016; Di Bella et al., 2022). On the other hand, the occurrence of violent gas outbursts or mudflows from active mud volcanoes may represent catastrophic event for benthic micro- and macro communities (Jerosch et al., 2007). Methane emissions from aquatic ecosystems are not well constrained due to the lack of observations and numerous uncertainties regarding the functioning of the associated ecosystems. The complexity of the interaction between different ecological factors characterizing the shallow fluid emissions makes it difficult to assess the pattern of biota responses *in situ*. Literature data have demonstrated the value of foraminifera as proxies for environmental characterization and for detecting contamination of seafloor ecosystems by methane (Dando et al., 1991; Gupta et al., 1997; Rathburn et al., 2000; Panieri, 2003; Portnova et al., 2014; Schwing et al., 2015; Yanko et al., 1999, 2017, 2023; Shnyukov and Yanko-Hombach, 2020). However, the influence of methane seepage on organisms is still poorly understood.

For example, published data have shown that it can have a positive, negative or null impact on meiobenthos (Dando and Hovland, 1992; Jensen et al., 1992; Polikarpov et al., 1998). However, little is known about its precise impact on infaunal and epifaunal living organisms. It is not clear if biogenic (Denman et al., 2007; Conrad, 2009; Schorn et al., 2022) or thermogenic (Meister et al., 2018) methane affect the microfaunal taxonomic and spatial distribution. Some researchers report a positive effect of methane on meio-benthic organisms, especially if they live directly on methane seeps (Luth et al., 1999; Rathburn et al., 2003; Wiedicke and Weiss, 2006; Panieri, 2006; Cook et al., 2011) where the development of microbial materials represents a further source of food for foraminifera. Similar results were observed from the fossil record in the Pacific Ocean during the Paleocene-Eocene Thermal Maximum (Thomas, 2003). Opposite findings were found at both shallow- and deep-water sites, where stressing conditions for the foraminiferal assemblages resulted in a decrease in faunal density and loss of biodiversity. In these environmental settings, the foraminiferal assemblages are always dominated by opportunistic species (Panieri, 2003; Pletnev et al., 2014). Likewise, a recent study in the Northwestern part of the Black Sea (Yanko et al., 2023) reached the same conclusions, showing lower simple diversity and abundance as well as smaller sizes of foraminiferal tests compared to those from areas not affected by hydrocarbon emissions, indicating that reproduction and growth strongly inhibited.

Other studies suggest that the occurrence of characteristic species or a specific composition of benthic foraminiferal assemblages may indicate methane release at the seafloor (e.g., Mackensen et al., 2006; Bernhard et al., 2009). This observation could be of great interest for paleoenvironmental reconstruction of the fossil record to investigate the relationship between methane and climate. For example, the release of methane from large marine reservoirs has been linked to climate change, both as a causal mechanism and as a consequence of temperature changes, during the Paleocene and Quaternary period (Rathburn et al., 2000; Panieri et al., 2014). One way to reconstruct past marine methane emissions is by carbon isotope ($\delta^{13}\text{C}$) analysis of benthic tests (e.g., Kennett et al., 2000; Panieri et al., 2016). Generally, depleted $\delta^{13}\text{C}$ values differentiate environments with methane venting activity from those that are not affected (Rathburn et al., 2003; Hill et al., 2004; Panieri et al., 2014). However, differences can also be caused by deep versus shallow environments and on the basis of local microhabitats. For example, the positive $\delta^{13}\text{C}$ signature of epifaunal taxa is due to the buffer

effect of photosynthesis activity, while in infaunal species the signature results are more depleted. Even if this strengthens the relationship between environmental conditions and ecological preferences of the different species (McCorkle et al., 1990, 1997; Rathburn et al., 1996, 2000), it shows the importance of a conservative approach when using this type of analysis.

In this work we report a study on benthic foraminiferal assemblages associated with active methane seepage offshore the Scoglio D'Affrica islet, along the Elba-Pianosa ridge in the northern Tyrrhenian Sea (western Mediterranean). On March 16th, 2017, a violent gas eruption occurred in this area, with the emission of a "dirty water" column rising up to 10 m above the sea level from a shallow-water mud volcano (Casalbore et al., 2020). So far, marine studies related to Scoglio d'Affrica have focused on the characterization of geomorphological (Motteran and Ventura, 2005; Spatola et al., 2023), geochemical (Meister et al., 2018; Saroni et al., 2020) and microbial (Ruff et al., 2016; Schorn et al., 2022) processes, while there is no information about the microfauna.

The aims of the present research are: 1) to determine the species composition of the benthic foraminiferal assemblages associated with shallow-water fluid emissions; 2) to assess the effect of fluid emissions on different microhabitats considering epiphytic, epifaunal and infaunal foraminifera; 3) to investigate the effect of methane on biomineralization processes; and 4) to provide new constraints on the ecological behavior of foraminiferal species in response to extreme conditions caused by methane release. These objectives aim to increase the knowledge on the microfaunal response in this extreme environment as a proxy to improve reconstructions of methane release in the past and better predict the impact of future climate warming on methane seepage.

2. Geological setting

The Scoglio d'Affrica islet lies in the southernmost part of the Elba-Pianosa ridge (northern Tyrrhenian Sea), a mainly submarine, north-south elongated morpho-structural high separating the Tuscany Shelf to the east from the Corsica Basin to the west (Fig. 1). The geological evolution of this area was related to the opening of the northern Tyrrhenian Sea due to the eastward rollback of the west-dipping Adria-Paleo-European subduction system (e.g., Carminati and Doglioni, 2012). Shallow marine Pleistocene calcarenites outcrop on Scoglio D'Affrica islet, lying above Triassic-Lower Jurassic limestones and the metamorphic basement (Cornamusini et al., 2002; Motteran and Ventura, 2005). The surrounding area was investigated by the oil and gas company AGIP in the 1970s through high-penetration seismic profiles and explorative work identified a thick succession of Eocene-Oligocene siliciclastic deposits together with gas pockets located at different stratigraphic levels within the turbiditic succession (Cornamusini and Pascucci, 2014). Widespread seafloor seepage has been reported by scuba divers since the 1960s, with a total gas flux rate estimated to be around 700 m³/day for the entire area (Del Bono and Giammarino, 1968; Barletta et al., 1969). According to these authors, the main gas was CH₄ (around 80%), with minor percentages of N₂, O₂, and CO₂. Recent gas sampling from active mud volcanoes identified in the study area also reported methane as the dominant gas component (approximately 96% of the total volume) and minor gases represented by carbon dioxide, nitrogen, ethane, and helium (Saroni et al., 2020). Based on $\delta^{13}\text{C-CO}_2$ and $\delta^{13}\text{C-CH}_4$ isotopic data, the methane is predominantly of secondary microbial origin (Meister et al., 2018; Saroni et al., 2020).

The general bathy-morphological setting of the study area (Spatola et al., 2023) highlights several fluid-related structures (i.e., several mud volcanoes and hundreds of pockmarks), morphological highs possibly related to piercement structures, escarpments, channels and bedforms. The detailed morphological characterization of the mud volcano responsible for the 2017 outburst (named Scoglio d'Affrica MV₁, SdAMV¹) is reported in Casalbore et al. (2020). It consists of two mounds

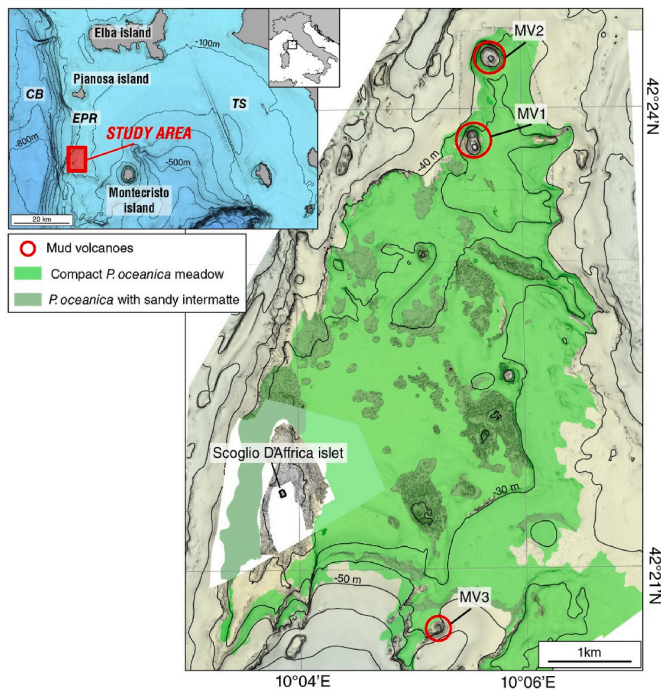


Fig. 1. Study area and bathymetric map of the Scoglio d'Africa (contour line spacing equals 10 m). The distribution of mud volcanoes and continuous and discontinuous *P. oceanica* meadows is from Spatola et al. (2023). Bathymetry in the upper left inset is obtained from Emodnet bathymetry (<https://emodnet.europa.eu/>); contour line spacing equals 100 m.

(M1 and M2) located at a water depth of approximately 10 m separated by a 15 m deep flat saddle. At the time of the measurements, the top of the southern mound was characterized by a smooth seafloor, covered by widespread mud breccia emitted by a 15–20 m wide ring-shaped crater, and diffuse seepage, as observed on videos collected using a Remotely Operated Vehicle (ROV). This smooth seafloor was surrounded by a blocky facies, except for the western flank where multiple mudflows were recognizable. The northern mound was dominated by a blocky facies at its top (except for small and confined smooth areas) and upper slope. The flanks of the mud volcano were generally steep (higher than 16° in the upper part) and smooth, except for the lower part characterized by a seafloor with small-scale roughness. This morpho-acoustic facies, groundtruthed by ROV observations, houses dense *Posidonia oceanica* meadows that are widespread down to –40 m depth and cover about 36% of the surveyed seafloor (Spatola et al., 2023). In some areas this facies laterally shifted to a dimpled morpho-acoustic facies, characterized by the presence of oval depressions that are a few metres to tens of metres wide and up to 2 m deep, corresponding to intermatte areas (i.e., sandy patches) that interrupt the continuity of the *P. oceanica* meadows. The interpretation of this morpho-acoustic facies agrees with previous studies, reporting dense sea grass meadows alternating with a seafloor floored by rhodoliths and bioclastic sand (Del Bono and Giammarino, 1968; Fravega and Vannucci, 1982; Cinelli et al., 1993).

3. Materials and methods

3.1. Sampling strategy

Three sampling surveys were carried out during May 2021, June 2022 and July 2023 in the depth interval 8–46 m. During the first survey, 11 seafloor samples and one *P. oceanica* sample (leaves and rhizomes, P4) were collected through grab sampling. Most were located at the top (G1, G9, G10, and G13) or along the flanks (G2, G7 and G11) of mud volcanoes. Three samples were collected inside (G3, G4, G5) and at

the edge (P4) of the intermatte areas within the dimple acoustic facies and one sample was retrieved from a morphological high along the western flank of the Elba-Pianosa ridge (G6) (Fig. 2, Table 1). The other two surveys were performed on the SdAMV₁ by scuba divers. A total of 9 seafloor samples and 3 *P. oceanica* samples were recovered at Mound 1 (M1: S1-S3, P1) and Mound 2 (M2: S4-S9, P2, P3) during the 2022 survey, while 6 seafloor samples (S10-S15) were collected only at Mound 2 (M2) during the 2023 survey (Fig. 2). The main advantage of using scuba divers was the possibility to perform targeted seafloor sampling at known distances from the main emission points in order to constrain the role of gas emissions in controlling foraminiferal assemblages. Unfortunately, the resulting sampling position is less accurate with respect to the grab samples. Scuba diver sampling was focused on two morphological settings linked to different venting activity: i) muddy sediments with a stronger emission activity and the local presence of gryphons or mudflows (Fig. 3a and b); and ii) muddy seafloor with weaker emission activity (Fig. 3c and d). Samples were collected at the point of weak leakage and 5–10 m away, at the top or flanks of the mounds.

Posidonia samples were similarly collected at the point closest to the emissions (about 5 m away) and at sites not affected by emissions. Such sampling strategy was planned to highlight potential differences in foraminiferal assemblages related to venting activity as well as to different substrates (sediment and sea grass leaves) (Table 1).

3.2. Grain-size analysis

Analyses were performed on all sediment grab samples (G1-G13), except for sample G4 due to its small volume. Analyses were carried out using dry sieving for the fraction coarser than 63 µm and a laser particle sizer for the fine-grained fraction (from 0.5 to 63 µm). Samples were pre-treated using hydrogen peroxide (20% solution) and distilled water to remove organic matter and salts. Samples were dried at 40 °C in a convection oven to obtain the dry weight and then the coarse fraction (gravel and sand particles >63 µm) was subsequently separated from finer silt and clay by wet sieving. The grain-size obtained for the coarse fraction was determined by dry-sieving at one-phi intervals (ASTM series), while the fine fraction was treated with 500 mL of distilled water and a 50 mL solution of sodium hexametaphosphate (Na₆[(PO₃)₆]) before analyzing with a laser particle sizer (Sympatec Helos LA). The descriptive statistics of grain-size distribution (mean, standard deviation, skewness, kurtosis) and sediments were classified according to the percentage of gravel, sand, silt and clay based on the Folk and Ward classification schemes (Folk and Ward, 1957).

Crystalline phases were identified using X-Ray Diffraction (XRD) on sample powder. Measurements were performed at the Department of Earth Sciences, Sapienza University of Rome (Italy) with a Bruker D500 diffractometer, using CuKα radiation ($n = 1.5418 \text{ \AA}$), operating at 40 kV and 40 mA, and at a step size of 0.025°.

3.3. Benthic foraminifera

Two sample types were sediment and *P. oceanica* (rhizomes and leaves). Different treatments were adopted for each following, as far as possible, the standard procedures (Langer, 1993; Schönfeld et al., 2012; Mateu et al., 2014).

Sediment (the upper 2 cm layer of the grab and scuba samples) was collected for benthic foraminifera analysis and stored in plastic containers. To distinguish the living fauna, all sediment samples were stained and preserved in a solution of 90% ethanol with 2 g/L of Rose Bengal (Walton, 1952; Lutze and Altenbach, 1991; Schönfeld et al., 2012). After 15 days, the samples were wet sieved through a 63 µm sieve and then dried at 40 °C. For each sample, living (stained) and dead foraminifera were counted, hand-picked, and identified using a binocular stereomicroscope. To detect living porcelaneous specimens, each test was broken. The Rose Bengal staining method has been widely used

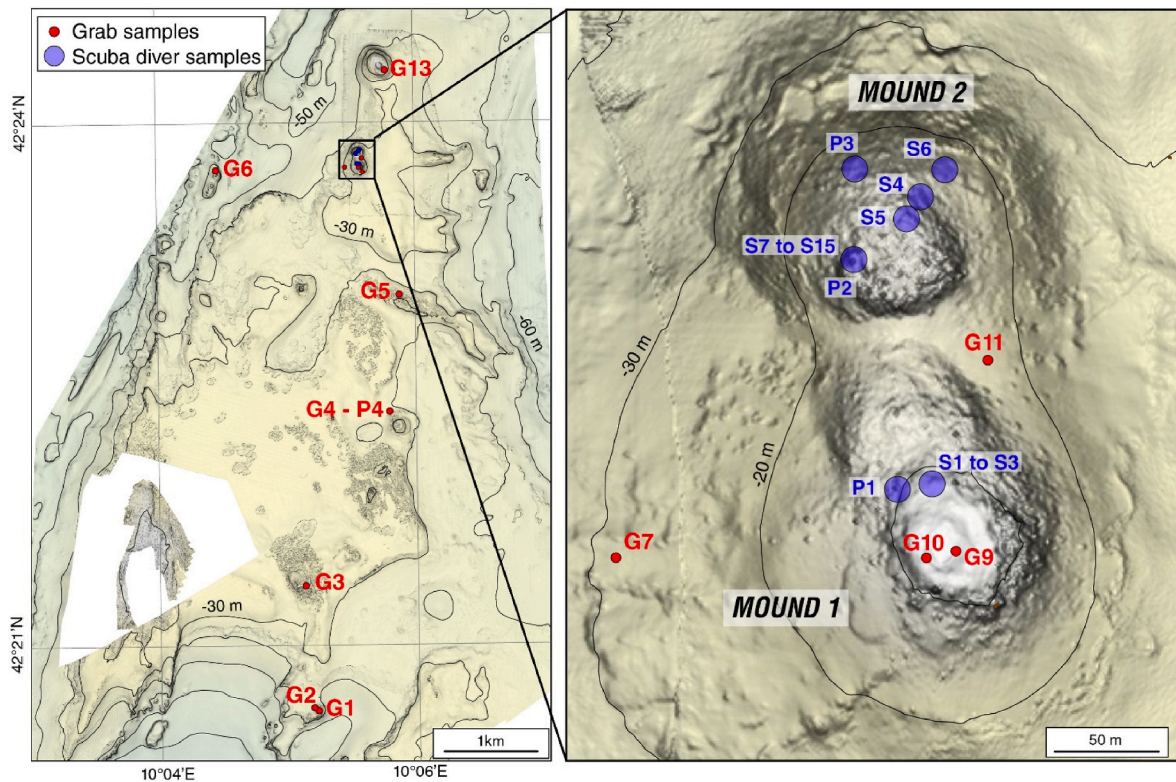


Fig. 2. Location of the sampled sites. The red dots denote the position of the grab samples collected in 2021, while the blue circles indicate the approximate areas where scuba divers collected sediment and *P. oceanica* samples in 2022 and 2023 on Mounds 1 and 2.

Table 1

Summary of sampling stations: grab and scuba sample ID, coordinates, depth and sample location EPR*: Elba- Pianosa Ridge.

Grab Sample ID	Lat	Long	Depth	Location
G1	42°20'37"N	10°05'13"E	28m	Top MV3
G2	42°20'38"N	10°05'11"E	33m	Flank of MV3
G3	42°21'20"N	10°05'08"E	21m	Intermatte zone
G4	42°22'20"N	10°05'47"E	28m	Intermatte zone
G5	42°23'00"N	10°05'53"E	25m	Intermatte zone
G6	42°23'44"N	10°04'28"E	46m	Flank of EPR* morphological high
G7	42°23'44"N	10°05'28"E	29m	Flank of MV1 (mud flow)
G9	42°23'44"N	10°05'34"E	8m	Top M1 (edge of the new crater) of MV1
G10	42°23'45"N	10°05'35"E	9m	Top M1 of MV1
G11	42°23'48"N	10°05'36"E	18m	Flank M2 of MV1
G13	42°24'17"N	10°05'46"E	17m	Flank of MV2
P4	42°22'20"N	10°05'47"E	28m	Edge Intermatte zone
Scuba Sample ID	Station area Lat	coordinates Long	Depth	Location
S1-S3	42°23'45"N	10°05'35"E	8m	Top M1 of MV1
S4	42°23'50"N	10°05'35"E	13m	Top M2 of MV1
S5	42°23'50"N	10°05'34"E	11m	Top M2 of MV1
S6	42°23'51"N	10°05'35"E	16m	Flank M2 of MV1
S7-S15	42°23'49"N	10°05'33"E	10m	Top M2 of MV1
P1	42°23'45"N	10°05'34"E	10m	Top M1 of MV1
P2	42°23'49"N	10°05'33"E	10m	Top M2 of MV1
P3	42°23'51"N	10°05'33"E	15m	Flank M2 of MV1

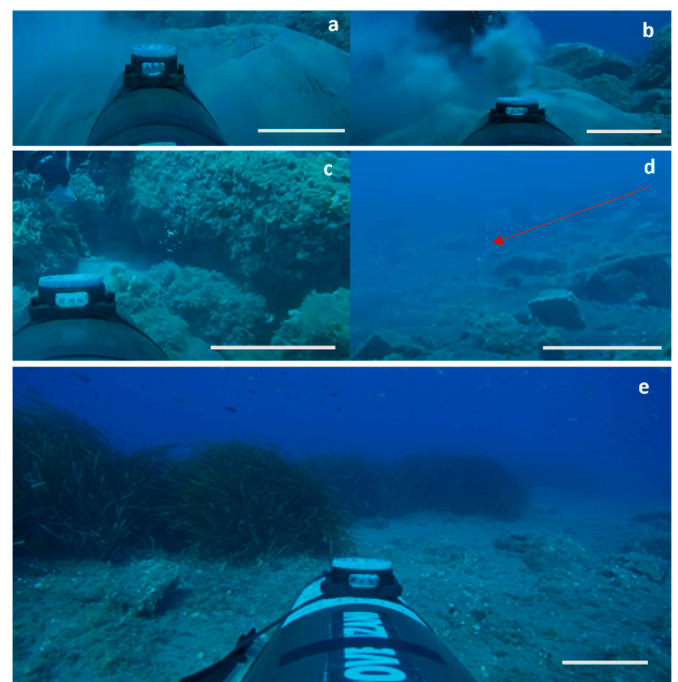


Fig. 3. a-b) Gryphons associated with a stronger emission activity (MV1); c-d); weak emissions (marked by a red arrow, MV1); e) *Posidonia* meadow along the flank of MV1. The white bar indicates an approximate reference scale of 20 cm. Photos by BigBlueExplorers.

in ecological studies to distinguish living from dead foraminifera because it is inexpensive and easy to use (Bernhard, 2000; Scott et al., 2001; Murray, 2006). However, under specific conditions (i.e., anoxic environments) the accuracy of this method may be affected by the presence of undecayed protoplasm, which can persist for weeks or months after death (Bernhard, 1988, 2000; Hannah and Rogerson, 1997;

Murray and Bowser, 2000). While the staining criteria are confidently applied to the superficial samples, ambiguities may arise in the case of deeper intervals (Fontanier et al., 2002), commonly consisting of a slight

overestimation of the living assemblages (Frontalini et al., 2018). In spite of this, the Rose Bengal method, when used with care, yields results that are as reliable as those obtained using other techniques (Lutze and Altenbach, 1991; Murray and Bowser, 2000; Figueira et al., 2012). The quantitative analysis of benthic foraminifera was based on the count of all specimens present in the whole sample. For the count of dead specimens, in order to prevent the inclusion of reworked or transported tests, only well-preserved tests that were not re-crystallized and were free of cracks and abrasions, were picked, counted and identified. The absolute abundance of living and dead foraminifera was calculated as the foraminiferal number (FN), defined as the number of specimens per gram of dry sediment (Schott, 1935). The species diversity, given by the H-index (Shannon, 1948) and as total number of taxa in the sediments (S), was calculated using the statistical package Palaeontological Statistics-PAST 4.13 (Hammer et al., 2001; Hammer and Harper, 2006).

P. oceanica samples –Two rhizomes and 3 to 4 leaves with similar lengths were analyzed for each site, resulting in a total of 10 rhizomes and 20 leaves. *P. oceanica* rhizomes were cut off from the substrate approximately 1 cm above the sediment surface. Leaves and rhizomes were immediately stowed in water-filled plastic bags and later carefully washed with seawater over a 63 μm sieve. Epiphytes were washed into larger bowls, washed with fresh water and dried. Plant fragments were examined under the microscope to remove living specimens that may have remained glued to the plant surface. All epiphytic foraminifera were picked from each sample and identified at the species level. The ratio between number of specimens recorded and number of leaves analyzed (F/P) was calculated to have a broad estimation of epifaunal density (Di Bella et al., 2022).

Genus-level classification was made according to the most used taxonomical study on foraminiferal genera (Loeblich and Tappan, 1987), while species were determined according to some important studies conducted in the Mediterranean area (Cimernan and Langer, 1991; Sgarrella and Moncharmont-Zei, 1993; Panieri et al., 2005) as well as the World Modern Foraminifera Database (Hayward et al., 2011). Some species were grouped for a better and more direct understanding of foraminiferal distribution patterns: rosalinids include *Neoconorbina* spp., *Gavelinopsis praegeri*, *Rosalina* spp. (see appendix) (Cimernan and Langer, 1991; Langer, 1993) muddy preference foraminifera include some Low Oxygen Foraminiferal Assemblages (Bernard and Sen Gupta, 1999) like *Bolivina* spp., *Bulimina* spp., *Fursenkoia acuta*, *Cassidulina* spp.; and the cibicides group includes *Cibicides refulgens* and *Lobatula lobatula* (Langer, 1993). The foraminiferal content was also analyzed on the agglutinated, porcelaneous and hyaline test. The quantitative data of the three tests were considered because the biomineralization can change as response to the physical and chemical seafloor conditions (Pettit et al., 2013; Di Bella et al., 2022; Yanko et al., 2023). To investigate the morphological, structural, and compositional characteristics of tests, Scanning Electron Microscope SEM, FEI Quanta 400, and Energy Dispersive X Ray Spectroscopy EDS measurements were made at the SEM Laboratory of the Earth Sciences Department, Sapienza University of Rome. A similar qualitative approach was used to examine the carbonate crusts that were found in most of the sediment samples.

The samples were attached to 12.5 mm SEM stubs using carbon tabs and then coated with a conductive layer (5–15 nm) of gold (Au) using an Emitech K550X sputter coater and a routine cycle time of typically less than 4 min. Samples were viewed in high vacuum mode using an accelerating voltage of 20 kV; the focus was adjusted to match the change in working distance (~11 mm) over the same range of the specimen and an improved image was obtained, ranging between 5 and 300 μm resolution.

3.4. Isotopic analyses

Three samples of *P. oceanica* (leaves), belonging to both near emissions and background sites, were analyzed for stable carbon isotope ratios and then compared with a sample belonging to the *P. oceanica*

meadows of Maratea (southern Italy), here used as a reference for an undisturbed, healthy environment.

To eliminate all the carbonate fraction belonging to the epiphytic organisms, the *Posidonia* samples were dipped in an 18% HCl solution for 10 s, abundantly rinsed with distilled water to stop the reaction and remove any trace of acid, and then dried at 40 °C.

Organic carbon isotope ratios ($\delta^{13}\text{C}_{\text{TOC}}$) were measured with a Finnigan Delta V Advantage Mass spectrometer coupled with a Flash 2000 Thermo Elemental Analyzer at the stable isotope laboratory of the Earth Sciences Department of Sapienza University of Rome. All the results were calibrated against the international standard Wheat Flour OAS. Analytical error is $\pm 0.2\text{‰}$ based on replicate standard analyses run together with the samples (N = 14).

3.5. Gas

Three gas samples were collected at different locations on the top of M2 on 18/07/2023. Bubbles were captured using an inverted funnel connected to a 1L glass ampule with inlet and outlet stopcocks and a gas sampling port. The funnel was held in place by a diver at a height of about 20 cm above the sea floor until the collected gas had displaced all seawater in the ampule. The samples were stored at room temperature and analyzed within 2 weeks using a Carlo Erba 8000 model gas chromatograph with helium carrier gas. Light hydrocarbons (C1 to C4) were separated on a 2m long CBK-BHT100 packed column and analyzed using a Flame Ionization Detector while carbon dioxide was separated on a 2m long Porapak-Q packed column and analyzed using a Thermal Conductivity Detector. Analytical reproducibility (1σ) is about $\pm 5\%$.

4. Results

4.1. Sediment characteristics

Two main types of sediments can be distinguished. The first group mainly consists of bioclastic sand and gravel recovered from intermatte areas on discontinuous *P. oceanica* meadows and on a morphological high in the western sector of the study area. The second group mainly consists of silty sediment with a variable proportion of gravel and cobbles, sampled at the top of the mud volcanoes or along their flanks (Fig. 4).

Sediments with a dominant bioclastic component (G3, G5, G6) consist of poorly to moderate sorted gravelly sands or sandy gravel, with a gravel content ranging between 19 and 47% and a silty/clayey content of <4% (Table 2). The inorganic sandy fraction is constituted mainly by quartz. The bioclastic fraction is characterized by fragmented and intact mollusks (bivalves and gastropods), bryozoans, serpulids, diatoms, echinoids, ostracods and foraminifera.

Sediments with fine- and coarse-grained fraction include heterogeneous sediment classes that range from gravelly mud to slightly gravelly sandy mud, all showing very poor sorting and coarse skewness, except for samples G1 (characterized by fine skewness) and G2 (with a symmetric distribution). The gravel and sand contents range from 1.4 to 13.2% and from 15 to 50%, respectively, while the fine-grained fraction (i.e. silt and clay) is between 45 and 80%. On the basis of diffractometer analyses, the coarser fragments are primarily carbonates (Mg-calcite and, to a lesser extent, Fe-(Mn)-bearing dolomite (ankerite), Fig. 5a). Carbonate gravels are held together by the fine-grained fraction, formed by prevailing clay minerals (kaolinite, montmorillonite, illite) and phyllosilicates (muscovite, chlorite) plus subordinate quartz (Fig. 5b).

SEM-EDS analyses show that some carbonate fragments have a concave crust morphology (Fig. 6A), which locally has an ankerite composition (Fig. 5A), while the matrix has a clay composition (Figs. 5B and 6B). The faunal content, which is very scarce, is represented by few specimens of bivalves and foraminifera. No bioclastic fraction is present.

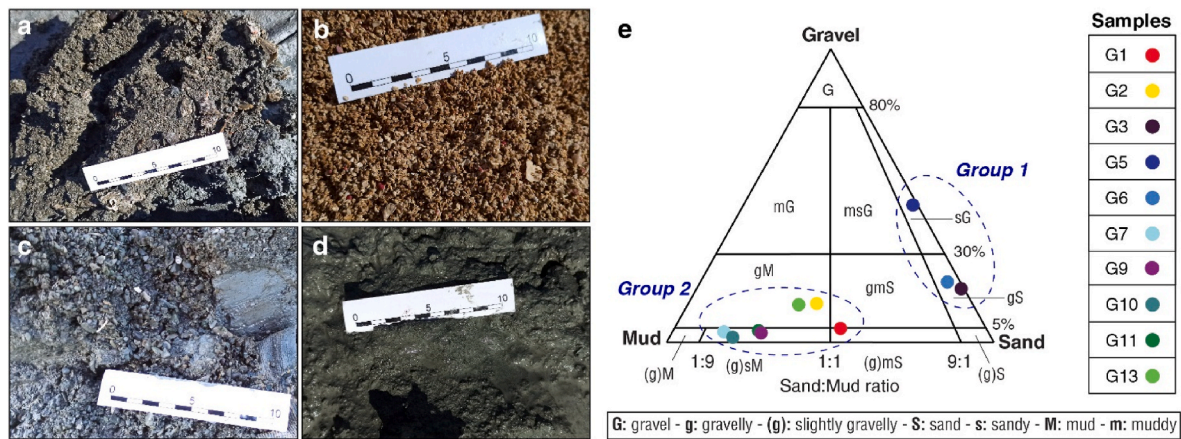


Fig. 4. Main types of sediment samples: a) G2: gravelly mud; b) G3: bioclastic gravelly sand; c) G7: slightly gravelly sandy mud (with higher gravel content); and d) G10: slightly gravelly sandy mud. e) Ternary diagram for the grab samples collected in 2021, showing the two main sediment types occurring in the study area. Sediment classification scheme from Folk and Ward (1957).

Table 2
Granulometric characteristics of sediment grab samples in the study area. (Slgr = slightly gravelly).

Sample	% Gravel	% Sand	% Silt	% Clay	Mean (phi)	Sorting	Skewness	Kurtosis	Folk Class
G1	4.96	49.79	25.17	20.08	4.43	3.31	0.25	0.76	(Slgr) Muddy sand
G2	13.19	39.46	24.15	23.2	3.95	4.08	0.06	0.78	Gravelly mud
G3	18.56	81.03	0.33	0.08	-0.55	0.58	-0.03	1.21	Gravelly sand
G5	47.72	51.74	0.44	0.1	-1.05	0.79	-0.16	1.08	Sandy Gravel
G6	20.89	75.93	1.94	1.24	0.23	1.53	0.13	1.03	Gravelly sand
G7	3.54	15.83	38.69	41.94	6.43	3.21	-0.59	1.53	(Slgr) Sandy mud
G9	3.99	27.19	37.3	31.52	5.83	3.34	-0.42	0.76	(Slgr) Sandy mud
G10	1.37	19.37	40.3	38.96	6.5	2.86	-0.49	1.05	(Slgr) Sandy mud
G11	4.02	26.35	40.42	29.21	5.81	3.25	-0.38	0.82	(Slgr) Sandy mud
G13	12.84	33.82	29.19	24.15	4.42	4.11	-0.27	0.69	Gravelly mud

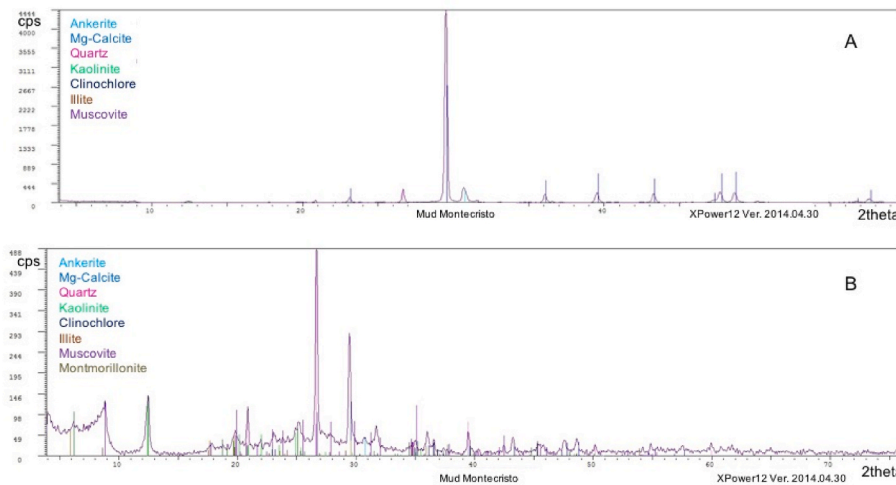


Fig. 5. X-ray diffraction pattern of a sample representative of the mineral assemblage constituting the carbonate clasts (A) and the muddy sediments (B).

4.2. Gas composition

Based on qualitative observations by the divers, bubble emission rates were significantly lower during the 2023 campaign when these samples were collected compared to that conducted in 2022. All gas bubble samples have a very similar composition (Table 3) that consists of about 95% methane, 350 ppm ethane, 4 ppm propane, 1% CO₂ and a CH₄/(C₂H₆+C₃H₈) ratio of about 3000. These values are very similar to those reported by Saroni et al. (2020) for samples collected in 2018 from bubble emissions in the same area. Gas flux rates, at standard

temperature and pressure conditions, are reported for two of the three points.

4.3. δ¹³C_{TOC} analyses

The δ¹³C_{TOC} of *P. oceanica* leaves in the Scoglio d’Affrica area ranges between -15.48‰ and -18.30‰, with the heaviest value recorded at a non-emission site (P3) and the lightest one at an emission site (P2). Conversely, the Maratea sample shows the heaviest C isotope signature of -13.63‰ (Table 4).

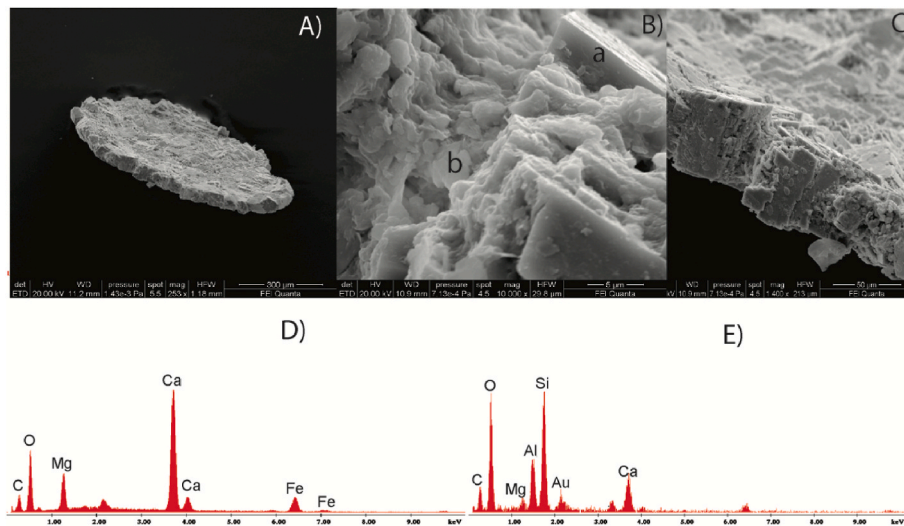


Fig. 6. SEM images of a carbonate crust (A); detail of carbonate crust (B): a) carbonate crystals and b) silicate matrix. C) Detail of the thickness of the crust; diatoms are visible. The related EDS spectra of a) and b) are given in D) and E), respectively.

Table 3

Gas concentrations of sampled bubbles. Note that gas flux rates are at Standard Temperature Pressure (STP) conditions. n/a – not analyzed.

Sample ID	CH ₄ (vol%)	C ₂ H ₆ (ppm)	C ₃ H ₈ (ppm)	CO ₂ (vol %)	C1/ (C2+C3)	Gas flux (ml/min)
B1	94.8	375	4.2	0.8	2500	200
B2	94.5	285	3.8	0.8	3272	30
C	92.8	350	3.9	1.1	2622	n/a

Table 4

Summary of $\delta^{13}\text{C}_{\text{TOC}}$ values of *P. oceanica* leaves from the study area (P1-P3 samples) and from a site not influenced by venting activity (MAR samples).

Sample ID	$\delta^{13}\text{C}$	Dev.St.P	$\delta^{13}\text{C}$ mean
MAR	-13.68		
MAR	-13.57	0.06	-13.63
P1	-17.04		
P1	-16.81	0.12	-16.93
P3	-15.51		
P3	-15.45	0.03	-15.48
P2	-18.43		
P2	-18.17	0.13	-18.30

4.4. Living and dead foraminiferal assemblages

Sediment samples - The foraminiferal content (living and dead assemblages) is widely variable across the study area (Fig. 7). Ten samples are totally barren (G1, G7, G10, G11, S1, S4, S5, S7, S14 and S15). In most samples the dead assemblage clearly prevails over the living one, except for G9 (M1), S8, S12 and S13 (M2) where the living specimens were dominant.

The dead assemblage includes a total of 109 species (Appendix). Agglutinated taxa are scarcely represented, being absent or with abundances <6% in most samples. In contrast, both the porcelaneous group and hyaline taxa are abundant, with values ranging from 15.91 to 79.46% and from 20.54 to 78.41%, respectively (Table 5).

The living (stained) assemblage includes a total of 84 species (Appendix). The agglutinated taxa are more frequent and diversified with respect to the dead assemblage, although they are totally absent in G6 and S2. The porcelaneous taxa are abundant with percentages ranging from 8.93 to 66.67%, except in sample G3 where they are not found. Hyaline taxa are dominant in all samples, similarly to the dead

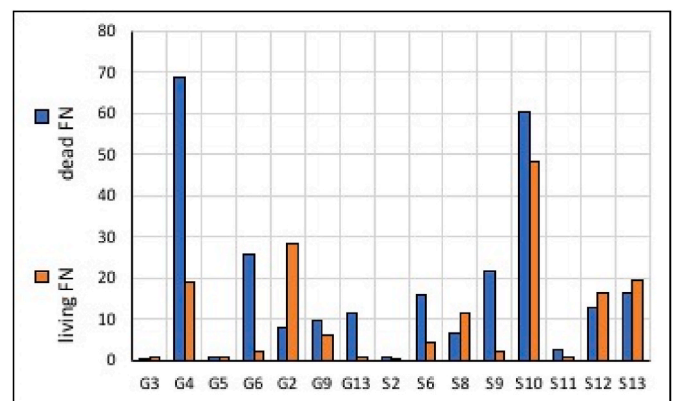


Fig. 7. Comparison of the density (FN = vertical axe) of living and dead benthic foraminifera in each sample.

assemblage, with percentages ranging from 33.33 to 84.62% (Table 6).

***Posidonia oceanica* samples** - *P. oceanica* leaves and rhizomes are characterized by the presence of encrusted organisms like serpulids, coralline algae, bryozoans and diatoms. The foraminiferal content consists of a total of 1233 individuals on all leaves and rhizomes. The diversity is higher on the leaves (mean value $H = 2.49$) than on the rhizomes (mean value $H = 1.43$). The highest density value for both rhizome and leaf samples was recorded in sample P4 (327.43 F/P), collected at the edge of an intermatte zone in the central sector of the study area, followed by sample P2 from the top of MV1-M2 (309.4 F/P) (Table 7). Although these values are similar, it should be noted that the foraminiferal content is mainly concentrated on the leaves in P2 (emission zone) and on the rhizomes in P4. The lowest F/P value is recorded in sample P3 near the top of MV1-M2 (99.71 F/P). Agglutinated taxa are very few or totally absent, both in the rhizomes and leaves, while porcelaneous species seem to mainly prefer the rhizome microhabitat. The hyaline specimens dominate both on leaves and rhizomes (Table 7, Fig. 8).

The list of observed species is reported in Appendix. Some species, like *Cibicides variabilis*, *Peneroplis* spp., *Miniacina miniae*, the most part of Miliolids and the agglutinated taxa, are recorded exclusively in the rhizomes. Rosalinids (*Neonorbina posidonicola*, *Gavelinopsis praegeri*, *Rosalina* spp.) are dominant both on the leaves and rhizomes, with

Table 5

Foraminiferal density (FN) and percentages of Agglutinated, Porcelaneous and Hyaline taxa, total number of individuals (N), number of taxa (S), diversity index (H) of dead assemblages calculated for each sample in which foraminiferal content was recorded. Barren samples are not reported.

Samples	FN ind/g	Agglutinated %	Porcelaneous %	Hyaline %	N	S	Shannon_H
G3	0.26	0.00	30	70	10	6	1.61
G4	68.79	1.48	20.2	78.33	205	34	2.72
G5	0.53	0.00	33.33	66.67	18	9	1.98
G6	25.70	4.00	27.43	68.57	175	38	3.19
G2	7.71	0.51	33.33	66.16	198	37	3.20
G9	9.69	5.68	15.91	78.41	88	36	3.27
G13	11.53	1.36	53.39	45.25	221	48	3.43
S2	0.66	0.00	62.5	37.5	48	17	2.38
S6	15.98	0.00	58.62	41.38	58	26	3.10
S8	6.27	0.00	66.67	33.33	75	29	3.00
S9	21.80	0.00	47.83	52.17	23	14	2.53
S10	60.19	0.00	78.65	21.35	192	41	3.41
S11	2.36	0.00	71.88	28.13	64	19	2.62
S12	12.79	1.40	61.54	37.06	143	40	3.25
S13	16.30	0.00	79.46	20.54	112	26	2.84

Table 6

Foraminiferal density (FN) and percentages of Agglutinated, Porcelaneous and Hyaline taxa, total number of individuals (N), number of taxa (S), diversity indices (H) of living (stained) assemblage calculated for each sample.

Samples	FN ind/g	Agglutinated %	Porcelaneous %	Hyaline %	N	S	Shannon_H
G3	0.90	60.00	0.00	40.00	30	6	1.47
G4	19.13	23.21	8.93	67.86	56	23	2.71
G5	0.50	33.33	13.33	53.34	15	10	2.12
G6	1.90	0.00	15.38	84.62	13	8	1.83
G9	28.41	5.43	38.75	55.82	258	46	3.22
G2	6.07	20.13	18.18	61.69	154	33	3.04
G13	0.73	10.00	50.00	40.00	10	6	1.70
S2	0.19	0.00	42.86	57.14	14	8	1.97
S6	4.13	6.66	26.67	66.67	15	9	2.06
S8	11.34	0.00	66.67	33.33	39	11	1.67
S9	1.91	14.28	42.86	42.86	7	6	1.75
S10	48.27	4.55	19.48	75.96	154	22	2.27
S11	0.63	1.39	36.11	62.50	72	20	2.61
S12	16.19	2.76	37.02	60.22	181	31	2.82
S13	19.21	0.76	30.30	68.94	132	24	2.53

the highest percentages at MV1 (M1 and M2).

Regarding the state of preservation, it should be highlighted that tests collected in the methane emission were poorly preserved. In fact, the SEM analyses highlight strong signs of cracks and fractures, resulting in increased shell fragility in all *P. oceanica* samples and leading to the formation of calcined shells (mainly in the miliolids and rosalinids tests) in the sediment samples. Moreover, in many cases the foraminifera are very small and have morphological alterations. Calcite crystals are also present in the samples collected near the emissions (Fig. 9).

4.4.1. Distribution of dead and living foraminiferal assemblages

The areal distribution of foraminiferal assemblages is described below according to the characteristics of the different sampling locations, which can be grouped into four main settings.

- (i) *Areas with strong emission activity, locally associated with gryphons and mud flows* – Samples collected in these areas (G1, G10, S1, S3 to S5, S7, S14 and S15) were totally barren of foraminiferal content. They were collected at or very close to the strongest emissions at the top of MV1 and MV3.
- (ii) *Mud flows along the flanks of MV1* – Similar to the previous samples, these (G7, G11) also lack microfauna, although no specific point emissions were detected at the time of sampling.
- (iii) *Muddy sediments associated with weak emissions* – Samples (S2, S6, S8-13, G2, G9, G13, P1, P2, P3) range from 0.19 to 48.27 ind/g for the living assemblage and 0.66 to 60.19 ind/g for the dead one (Tables 5 and 6). The living specimens are only dominant in the samples collected at MV1 (M1: G9 and M2: S8, S12, S13). In

the dead assemblage, the agglutinated taxa are absent in most samples. The highest percentage (5.68%) is recorded in sample G9. The presence of *Eggeroloides advenus*, *Lepidodeuterramina ochracea*, *Reophax* sp. and *Textularia* spp. is scarce. The porcelaneous group is abundant, with percentages ranging from 15.91 to 79.46%. In most MV1 samples, these taxa are >40%. The most common species are miliolids (*Adelosina* spp., *Quinqueloculina* spp., *Triloculina* spp.) and *Peneroplis* spp. (Appendix). Hyaline taxa range from 21.35 to 78.41%, with values > 30% in all samples except for S10, S11 and S13 (MV1) (Table 5). The most common are rosalinids and cibicids, which are associated with other typical shallow water taxa like *Buccella frigida*, *Elphidium* and *Glabratella* spp. (Appendix). The diversity index (H) values are always >2, ranging from 2.38 to 3.43.

For the living assemblage, the agglutinated taxa represent 20.13% and 14.28% in G2 and S9, respectively, but are absent or scarcely represented in the other samples. The porcelaneous group is frequent, ranging from 18.18% to 66.67% in most samples. *Quinqueloculina stelligera* is the most abundant species (mean value 9.07%) with the maximum abundance recorded in samples G13, S8 and S9 (Fig. 10). However, at the top of M1 (MV1: G9), high frequencies of *Affinetrina gualtieriana*, *Siphonaperta aspera*, *Quinqueloculina boschiana* and *C. involvens* are recorded. Hyaline taxa are dominant in all samples, similar to that recorded in the dead assemblage, with percentages ranging from 33.33% to 68.94%. Overall, the living assemblage reflects the composition of the dead one. Rosalinids and miliolids represent the most abundant taxa, with mean percentages of 27.52% and 24.20%,

Table 7
Quantitative data expressed as total number of individuals (N), specimens of Agglutinated (Aggl.), Porcelaneous (Por) and Hyaline (Hyal) taxa, counted on the *P. oceanica* samples. Foraminiferal density is expressed as number of individuals recorded on rhizomes and leaves analyzed (F/P ratio). Foraminiferal diversity expressed as number of taxa (S), Shannon (H).

Sites	Leaves					Rhizomes					Sediments					
	Samples	N	S	H	F/P	Samples	N	S	H	F/P	Samples	N	S	H	F/P	
M2	P2	298	24	2.78	0	294	78	12	1.37	309	S8	39	11	1.67	0	13
M2	P3	94	9	1.91	0	94	40	7	1.07	99	S9	7	6	1.75	0	4
M1	P1	178	16	2.33	0	173	65	13	1.64	187	S2	14	8	1.97	0	8
Edge Intermatte	P4	178	42	2.93	1	173	302	10	1.65	327	G4	56	23	2.71	13	38

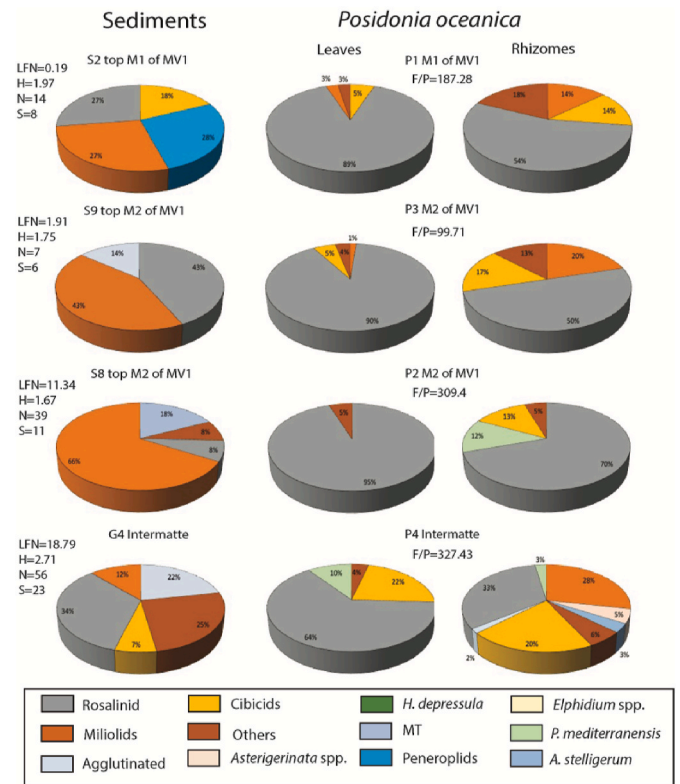


Fig. 8. Pie diagrams showing living foraminiferal assemblage recorded within sediments, leaves and rhizomes at the different study sites. The most abundant taxa are reported in the legend. Sediment samples collected at or as close as possible to the *Posidonia* samples are reported. (FN = density expressed as Foraminiferal Number in the sediment samples; H= Shannon index; N = number of total specimens; S = number of taxa; F/P = density expressed as total number of specimens recorded in leaves and rhizomes).

respectively. Among these, *G. praeegeri* (mean abundance 13.82%) prevails in the former, occurring in most samples except for G13, S10 and S11 where it is replaced by *Rosalina* spp. *Posidonia* assemblages (P1-P3) are dominated by rosalinids too (Fig. 8). It should be noted that these typical shallow water taxa are associated with high percentages of *Bolivina* spp. These taxa are most common in the muddy sediments at the top of M2 (MV1: S8, S10-S13), with values ranging from 14.92% up to 37.88% (Fig. 10) and at the edge of M1 (18.22%, MV1: G9). Sometimes (G9, S12, S13) they are associated with frequent *Haynesina depressula* and very small specimens of *G. praeegeri*. Shannon index (H) values range from 1.67 to 3.22, however it should be highlighted that the low values (<2) are recorded where the number of living specimens is minimum (Table 6).

(iv) Intermatte areas or morphological highs on the EPR flank (G3, G4, G5, G6, P4) - The samples retrieved from the intermatte zones and on the EPR flank (G3-G6) have faunal density (FN) values ranging from 0.50 to 19.13 ind/g for the living assemblage and between 0.26 and 68.79 ind/g for the dead one (Fig. 11). Except for G3, the dead assemblage clearly prevails over the living one in all samples. The H-index in both assemblages are very similar, with mean values of about 2. In the dead assemblage, the agglutinated taxa are characterized by carbonate cement (*Textularia bocki*) and a random occurrence, with maximum levels in sample G6 (4%). The porcelaneous group is well represented with values ranging from 20.20 to 33.33% (Table 5). Hyaline taxa show abundance percentages from 66.67 to 78.33%. Rosalinids and *Lobatula lobatula* are the dominant species followed by

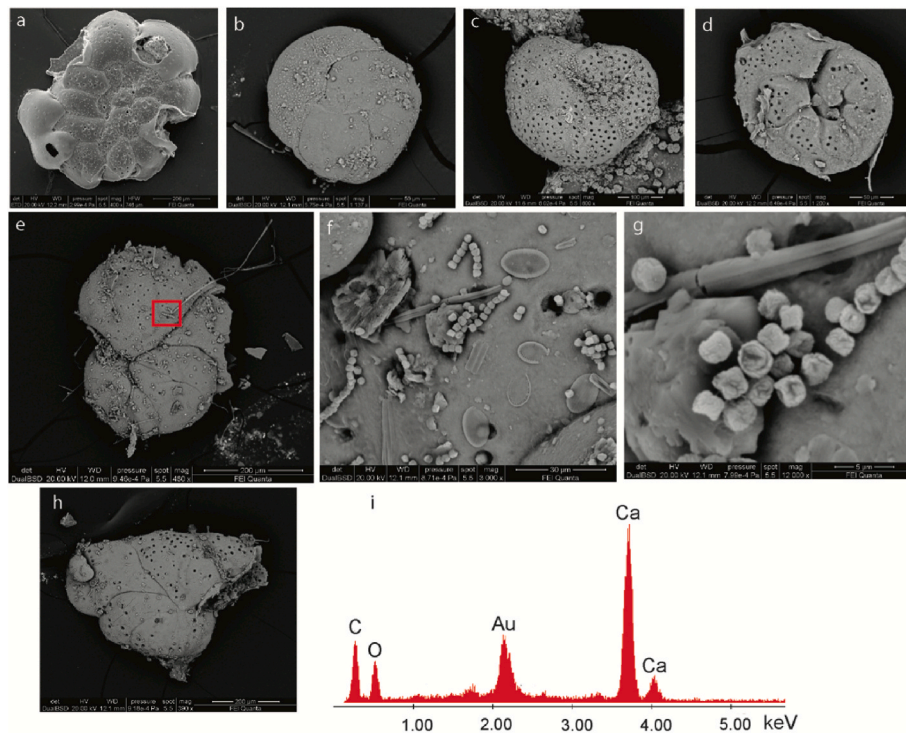


Fig. 9. SEM images of some species from *P. oceanica* samples. a) *Planorbulina mediterraneensis* (P3 sample); b) *Neconorbina posidonicola* (P1 sample); c) *Rosalina bradyi* surface view (P3 sample); d) *R. bradyi* apertural view (P3 sample); e-i) *Lobatula lobatula* (P3 sample): e) the red square shows calcite minerals; f-g) details of calcite minerals developed on the test surface; i) spectrum resulted from EDS analysis of the calcite minerals. All specimens show morphological variations, mainly in pore size and distribution; cracks and fractures affecting the chambers are also visible.

Asterigerinata spp., *Planorbulina mediterraneensis* and *Elphidium* spp.

The living assemblage is characterized by more frequent and diversified agglutinated taxa (23.21–60%) with respect to the dead one, however they are totally absent in G6 (Table 6). The most representative species, like *Ammodiscus planorbis*, *L. ochracea* and *Ammoglobigerina globigeriniformis*, lack carbonate cement (Fig. 12). The porcelaneous taxa are scarcely represented with levels ranging from 8.93 to 15.38%, except for sample G3 where they are totally absent. *Quinqueloculina* and *Triloculina* are the most representative genera. The hyaline taxa are the most abundant (40–84.62%) (Table 6). Among these, rosalinids (*Rosalina* spp. and *G. praegeri*) is the only dominant group.

The *Posidonia* sample (P4) records the highest values in F/P ratio and biodiversity (H-index, Table 7).

5. Discussion

5.1. Response of foraminiferal assemblages to CH₄ emissions

The analysis conducted at sites exposed to different degrees of CH₄ emissions around Scoglio d'Affrica allows us to make some considerations regarding the impact of this gas on the distribution, faunal density and biodiversity of foraminiferal assemblages. It is worth noting that while in deep-sea venting settings the environmental conditions are typically more homogeneous and support assemblages that are poorly diversified and mainly constituted by infaunal low-oxygen taxa (Rathburn et al., 2000; Panieri, 2003; Yanko et al., 2023), in shallow waters the higher partitioning of the microhabitats makes it more difficult to define a pattern of biota response and to identify seep-specialist taxa. Moreover, different from deep water seeps, shallow-water venting environments are also influenced by the input of photosynthetic carbon due to the presence of vegetal cover (Levin,

2005), leading to assemblages that are formed by the mixing of typical oxic, sandy, shallow-waters taxa with muddy, low-oxygen-tolerant taxa (MT).

Other aspects to be considered are the time of exposure of the benthic microfauna to the emissions and the seep intensity, factors linked to the temporal variability of the venting activity (Geistdoerfer et al., 1995; Shank et al., 1998). The resilience and recolonization capability of each species following environmental changes, however, can significantly determine the observed microfaunal distribution. In our case, the presence of methane emissions in the area has been known for at least 60 years, suggesting a relatively long-lasting impact on the seabed, although the intensity of emissions and their spatial distribution can vary over short time scales (annually or monthly). This may explain the wide variability of assemblages (composition, density and diversity) highlighted in this study. Moreover, the presence of typical morphological (mud volcanoes, pockmarks, gryphons and mud flows) and sedimentological (muddy sediments) fluid seepage indicators, along with widespread bacterial mattes and authigenic Mg-rich carbonate crusts, testifies to a consolidated, long-term venting activity.

Our data show that the processes linked to the methane emissions exert a strong influence on the characteristics of foraminiferal assemblages. Indeed, the emission of mud breccia mainly associated with mud eruptions (mudflows or violent gas outbursts like the 2017 event), as well as the formation of small gryphons produced by sustained emissions, represent very anomalous conditions for shallow-water benthic foraminiferal communities that are mainly adapted to a sandy substrate with an epifaunal style of life. It is possible that the mud leakage represents an additional stressor in addition to that due to methane emissions. However, our data do not allow us to distinguish whether the effect of CH₄ seepage is more or less influential than the mud emplacement. The impacts of these two stressing factors are highly variable at a small spatial scale, resulting in a complex interplay between local abiotic and biotic factors.

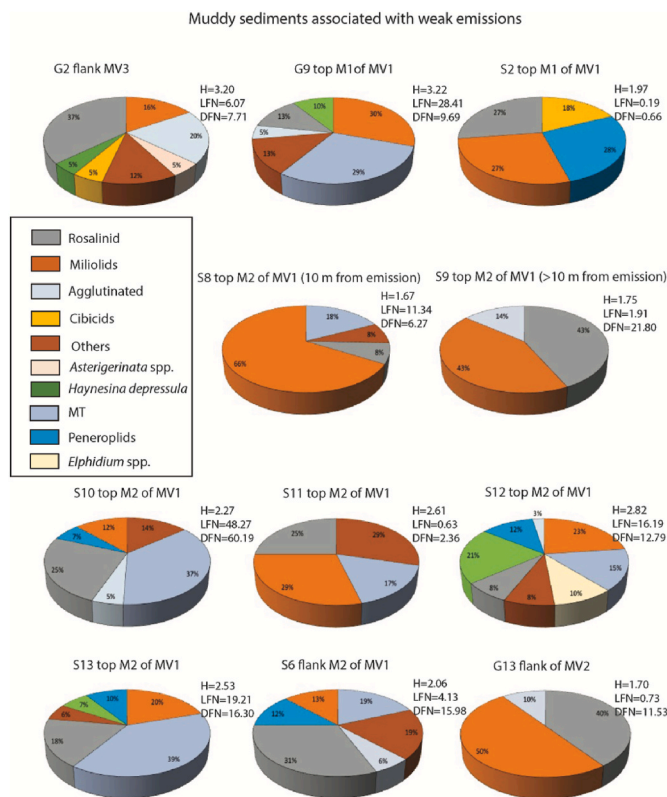


Fig. 10. Pie diagrams showing the living foraminiferal compositions in muddy sediment samples collected near weak emissions (Living foraminiferal density = LFN; Dead foraminiferal density = DFN; H= Shannon index; MT = muddy preference taxa).

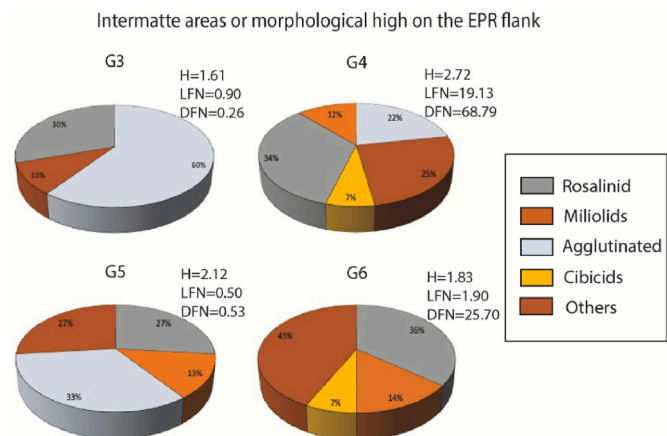


Fig. 11. Pie diagrams showing the living foraminiferal compositions in the sediment samples collected in the intermatte areas (Living foraminiferal density = LFN; Dead foraminiferal density = DFN; H= Shannon index).

Considering the morphological characteristics of the seafloor, linked to different degrees of venting activity, we can detect 5 different distribution patterns on and off the mud volcanoes.

- (i) *Areas with strong emission activity at the top of the MV, locally associated with gryphons and mud flows* – These are commonly characterized by fluffy muddy sediments on which the development of foraminiferal communities is strongly inhibited. Similar to other organisms (Levin, 2005), the direct exposition to methane and/or mud leakage may not be conducive for

colonization by propagules (very small individuals <32 µm, in a resting stage), thus hindering the start of biomineralization and/or agglutination processes (Alve and Goldstein, 2010) both on and inside the seafloor. Moreover, the presence of abundant fragments of authigenic carbonate crusts suggest probable hostile conditions for foraminiferal life. Indeed, the precipitation of authigenic carbonates observed in these areas is favored by methane oxidation presumably coupled to sulphate reduction at the water/sediment interface. This process can potentially result in extremely high concentrations of hydrogen sulphide, release of CO₂, decrease of pH and severe depletion or absence of O₂ immediately below and at the sediment/water interface (Gupta et al., 1997; Levin, 2005; Kravchishina et al., 2021).

- (ii) *Mud flows along the mud volcano flanks* – The anomalous absence of foraminiferal content along the flank of MV1, where emissions are not actually recorded, should be highlighted. A possible explanation for this observation is that overlapping mudflows may create strong anoxic microhabitats that inhibit foraminiferal colonization and development. In this case, the absence of life is probably due to the impact of the mudflows on the sea bottom rather than the methane emissions.
- (iii) *Muddy sediments associated with weak emissions* – In some locations, weak emissions are recorded on sandy muddy sediments or among sparse blocks, with intermittent bubbling not associated with any particular morphological structure.

In this environmental setting, microfauna presents different living/dead ratios depending on the time of colonization by each species. In more detail, the samples characterized by a greater living than dead assemblage (G9, S8, S12, S13) indicate a new phase of colonization, whereas where the dead content dominates the colonization was already under way thus reflecting more normal marine conditions (G13, S2, S6, S9-S11). In both cases, living and dead assemblages are characterized by the presence of infaunal muddy preference taxa, like bolivinids, that are well adapted to scarcely oxygenated bottoms (Gupta and Machain-Castillo, 1993; Bernhard et al., 1997; Bernhard and Sen Gupta, 1999). At the species level, *Bolivina variabilis* (probably corresponding to the Norwegian *B. pseudopunctata*, Alve and Goldstein, 2010) and *B. pseudoplicata* show a better adaptation to seep environments, similar to deep water conditions, thus confirming their opportunistic behavior (Armynot du Châtelet et al., 2011; Jorissen et al., 2018; Bouchet et al., 2021). These species have been observed in European oxygen-depleted bottom waters from the Mediterranean to the Norwegian Sea (Murray, 2006), like in deep Norwegian fjords (Kuhnt et al., 2007; Alve and Goldstein, 2010; Schmiedl et al., 2003). These species are the only ones we find in our study that also occur in a deep environment (Rathburn et al., 2000; Yanko et al., 2023). Their infaunal way of life (including their tolerance to low oxygen and organic-matter-rich environments) probably favors their adaptation to seep conditions. In samples S11, S12, S13 and G9, bolivinids are sometimes associated with high levels of *H. depressula*, infaunal taxon tolerant to high organic carbon concentrations and that likely feed on bacterial mats (Murray, 2006; Panieri, 2006; Armynot du Châtelet et al., 2011). Amongst the miliolids, *Quinqueloculina stelligera* seems to be the species that is most tolerant to the emissions, although experimental data show this species to be sensitive to long-lasting anoxia in the presence of hydrogen sulfide (Langlet et al., 2014). Its occurrence in fine sediments agrees with data coming from the Tyrrhenian Sea (Celia Magno et al., 2012; Mendes et al., 2012), while controversial behavior of this species is reported in the presence of environmental stressors like pollution, organic carbon or anoxia (Romano et al., 2009; Buosi et al., 2012; Langlet et al., 2014; Sreenivasulu et al., 2019). Amongst the rosalinids, *G. preageri* and *R. bradyi* are the species that are more tolerant to stressing conditions. They are two epifaunal taxa which can live on a wide range of sediment types and depths. In particular, the former may be recovered from inner shelf to deep basin waters (Sgarrella and Montchamont-Zei, 1993; de Stigter

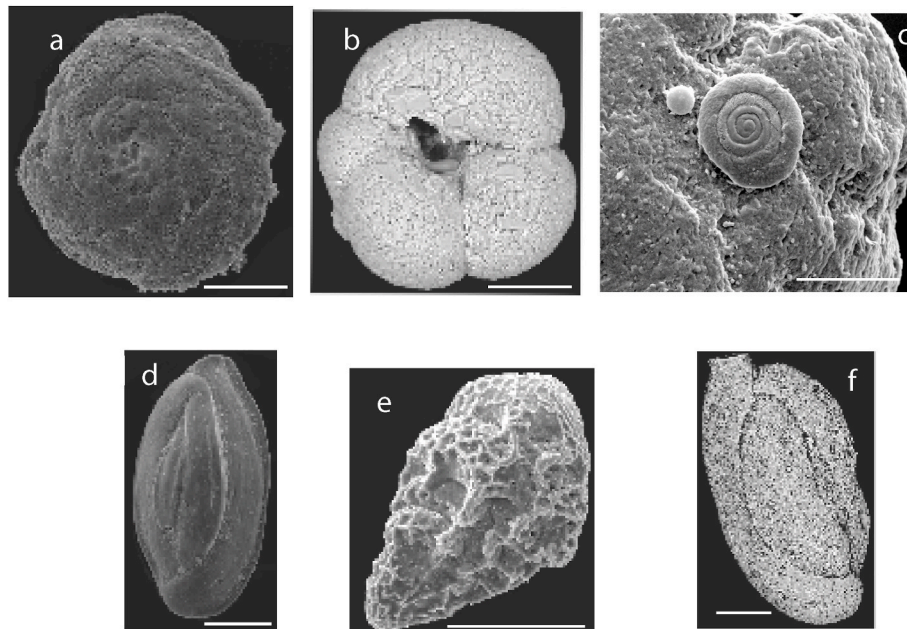


Fig. 12. SEM images of some foraminiferal specimens recorded in the samples from the intermatte areas or morphological highs on the EPR flank: a) *Lepidodeuterammina ochracea* side view (sample G3); b) *Ammoglobigerina globigeriniformis* apertural view (G4 sample); c) *Ammodiscus planorbis* side view (sample G4); d) *Quinqueloculina stelligera* side view (sample S8); e) *Bolivina pseudoplicata* side view (sample S10); f) *Siphonaperta aspera* side view (sample G9). The bar corresponds to 100 μm .

et al., 1996; Murray, 2006; Bergamin et al., 2018) whereas *R. bradyi* has exhibited a high tolerance to natural and anthropogenic stressors (from in situ and laboratory experiments), showing a greater adaptability to future warming (Damak et al., 2020), high eutrophic environments (Romano et al., 2021), pH fluctuations (Ramajo et al., 2019) or other extreme environments (Lei et al., 2015).

(iv) *Intermatte zones associated with bioclastic sediments without emissions*– (G3-G6). These samples are located outside of the active MV and are not presently affected by methane emissions. The absence of muddy sediments suggests no recent leakage of mud and presumably no methane emissions. The ratio of dead and living assemblages reflect normal marine conditions with the dominance of dead taxa and the absence of muddy preference taxa. In this case, it is reasonable to think that higher values of dead association are due to the sum of many generations while the living assemblage represents only the time of sampling (linked to patchiness and seasonality) (Murray, 1991). Only one sample (G3) shows microfaunal features that are more similar to that recorded in samples collected in the areas with weak emissions. From a compositional point of view, the assemblages of these samples (included G3) are characterized by typical shallow water taxa belonging to cibicides, rosalinids and miliolids, indicative of well-oxygenated conditions and high hydrodynamism.

(v) *Posidonia rhizomes and leaves* - The distinction between leaves and/or rhizomes microhabitats allows us to speculate not only on the microhabitat preference of foraminifers at the species level but to also highlight their functional aspect. The intermatte area and its edges (P4) can be considered as being representative of normal marine conditions, recording healthy leaves and high epiphytic diversity and density for the whole rhizomes and leaves, similar to that observed on the surrounding sediments (G4). However, it is to note that density and diversity recorded in intermatte area and its edges (P4) are lower than those recorded in other Mediterranean *Posidonia* meadows not affected by venting activity (Langer, 1993; Mateu-Vicens et al., 2014 and referen). This may be due to a possible indirect influence of the emissions. The decrease in density and diversity recorded in the

rhizomes coming from the emission areas (P1-P3) indicate a negative impact probably due to the vicinity of fluid leakage. A comparison between leaves, rhizome and sediment assemblages show similar patterns (Table 7, Fig. 8). The leaf assemblages are more abundant and diversified, testifying that this elevated microhabitat provides better life conditions than the rhizomes and sediments. Different from other venting activity areas, where rhizomes can act as “refugia”, in this case leaves can offer “elevated” substrates (e.g., Linke et al., 1993; Schönfeld, 1997; Schönfeld, 2002) on which suspension feeders can better exploit nutrients in the surrounding water mass, a greater degree of oxygenation and probably a better advantage of the *Posidonia* buffer effect (Langer, 1993; Baruffo et al., 2021; Buosi et al., 2012; Di Bella et al., 2022). Very little is known about the relationship between methane and its effect on *Posidonia* productivity. Although our results do not highlight a clear relationship between emissions and epiphytic assemblages, it is possible that *P. oceanica* meadows have an indirect buffer effect in the presence of CH_4 emissions, like that demonstrated for CO_2 emissions both in situ and during laboratory experiments (Vizzini et al., 2010; Ramajo et al., 2019; Di Bella et al., 2022; Capó-Baucà et al., 2023). The slightly more depleted isotope values obtained from the *P. oceanica* samples near the emissions may be due to its capability to sequester CO_2 by mean of photosynthesis. Although CO_2 concentrations in the gas bubbles are relatively low (Table 3), values may increase in the dissolved phase due to methane oxidization process favored by the well-oxygenated water characterizing the study site. Moreover, the methane stored inside the first centimeters of seafloor could be oxidized by the microbial activity, or enhanced respiration could take place in the nutrient-rich muds, thus increasing the CO_2 concentrations in the sediments where *Posidonia* have their roots (Knittel and Boetius, 2009; Herguera et al., 2014; Li et al., 2021). From a compositional point of view, the increase of rosalinids in both microhabitats (leaves and rhizomes) of *P. oceanica* samples near the emissions confirms their opportunistic behavior to the detriment of miliolids. Although in normal conditions miliolids are considered opportunistic taxa well-adapted to stressful

conditions (Langer, 1993; Mateu-Vicens et al., 2014 and referen), the low frequencies recorded in this site can be due to the high Mg-calcite test composition that make them more susceptible to dissolution in acidic conditions (Dias et al., 2010; De Nooijer et al., 2009). This result appears to be confirmed by data obtained from other venting sites like Aeolian Archipelago (Di Bella et al., 2022).

Impact on biomineralization processes and morphological abnormalities - Evident morphological abnormalities with reduced biomineralization is observed in the foraminifer tests, both in sediments and *P. oceanica* samples. This is very similar to the poor state of shell preservation recorded at sites with strong CO₂ emissions that lower the pH and acidify the waters. Studies from in situ observations and experimental data indicate critical threshold pH values around 7.8 and 7.6 that limit the building of carbonate tests (Dias et al., 2010; Pettit et al., 2013). Di Bella et al. (2022) report similar test fragility at pH values ranging between 7 and 8, in foraminifera from sites off Panarea Island (Eolian Archipelago). In our case-study, although the CO₂ content in the bubbling gas is low (Table 3) it may be sufficient to decrease pH values and inhibit test calcification. This mechanism may justify the poor preservation state of the tests. Moreover, some morphological abnormalities, like increased pore size and their inhomogeneous distribution on the dorsal surface observed on some recovered epifaunal specimens (*L. lobatula*, *P. mediterraneensis*, *R. bradyi*), may represent additional evidence of stressed environmental conditions. The epifaunal taxa are generally adapted to well-oxygenated environments and usually exhibit pores on the dorsal surface of the tests for gas acquisition and respiration (Leutenegger and Hansen, 1979; Bernhard et al., 2010; Glock et al., 2012). Size and number of pores on benthic foraminifera from oxygen-poor environments tend to be higher than those of specimens from well-oxygenated habitats (Rathburn et al., 2018 and referen). Thus, variations of the dissolved oxygen content may cause morphological pore abnormalities. In our case, the increase of the pore sizes against a decrease in their number on the surface of the chambers may be linked (directly or indirectly) to the emissions, similar to morphological abnormalities observed in specimens living in other venting sites. However, their relationship with the dissolved oxygen content is still difficult to establish. For example, whereas pore abnormalities recorded in the infaunal taxa could be due to oxygen variations because they live inside the sediment where oxygen depletion is conceivable, it is more difficult to explain their occurrence on specimens from vegetal microhabitats where the intense hydrodynamics and photosynthetic activity should yield a well-oxygenated environment.

6. Conclusions

The analysis conducted at sites affected by CH₄ venting activity around the Scoglio d'Affrica allow us to make some considerations on benthic foraminiferal response to these gas (±mud) emissions in shallow water environments. Our data show that there is a strong influence of the sedimentary processes linked to the methane emissions on the foraminiferal assemblages, resulting in a very patchy spatial distribution of foraminiferal assemblages linked to complex abiotic and biotic interactions. On the basis of our observations, methane emissions and mud emplacement represent the two main stressor factors for the benthic foraminiferal assemblages. At present, it is not possible to define whether the effect of CH₄ is more or less influential than mud emplacement.

Considering the morphological characteristics of the seafloor linked to different degree of venting activity, 5 different settings on and off the mud volcanoes were detected, associated with distinct characteristics of the microfaunal assemblages.

- 1) Areas with strong emission activity at the top of MVs, locally associated with gryphons and mudflows, where the environmental conditions are clearly prohibitive for foraminiferal life.
- 2) Mud flows along the flanks of mud volcanoes, where overlapping mudflows probably have a negative impact on life development, leading to barren sediments.
- 3) Muddy sediments associated with weak emissions where the development of the foraminiferal community is favored, although with differences in terms of density, diversity and compositional features linked to time of colonization by each species. In this setting, infaunal taxa (boliviniids) are favored to rapidly colonize muddy, poorly oxygenated sediments linked to the emissions. Among miliolids, *Q. stelligera* seems to be the most tolerant together with rosalinids (mainly *R. bradyi* and *G. praegeri*) and the hyaline taxa *H. depressula*.
- 4) Intermatte zone under scarce or absent emissions, characterized by typical shallow water taxa belonging cibicides, rosalinids and miliolids and indicative of well-oxygenated conditions and high hydrodynamism.
- 5) *P. oceanica* substrates, characterized by higher foraminiferal content on leaves compared to the rhizomes and surrounding sediment samples. In venting zones, *P. oceanica* leaves potentially offer "refugia" to epifaunal taxa that generally live on the seafloor under normal marine conditions. Similar to the surrounding sediment samples, the epiphytic assemblages are dominated by rosalinids, showing them to be a highly resilient taxa with an opportunistic behavior.

Many questions still remain open concerning the relations and influences of methane on the benthic associations in shallow water environments. Although it is difficult to define a pattern of biota response and to identify seep exclusive taxa, benthic foraminifera can represent good environmental proxies for both monitoring the variability of recent venting activity and detecting stressed conditions occurring in the geological record. The seafloor around Scoglio d'Affrica may represent a very promising study site for multidisciplinary marine research regarding venting activity, geochemistry of cold seep fluids and their effects on benthic organisms.

CRediT authorship contribution statement

Letizia Di Bella: Writing – review & editing, Writing – original draft, Supervision, Methodology, Investigation, Data curation, Conceptualization. **Martina Pierdomenico:** Writing – review & editing, Writing – original draft, Methodology, Investigation, Data curation, Conceptualization. **Aida Maria Conte:** Writing – review & editing, Writing – original draft, Methodology, Investigation, Conceptualization. **Irene Cornacchia:** Writing – review & editing, Writing – original draft, Methodology, Investigation, Data curation, Conceptualization. **Tania Ruspandini:** Writing – review & editing, Writing – original draft, Methodology, Data curation. **Daniele Spatola:** Writing – review & editing, Writing – original draft, Methodology, Investigation, Data curation, Conceptualization. **Stanley Eugene Beaubien:** Writing – review & editing, Writing – original draft, Supervision, Methodology, Investigation, Data curation, Conceptualization. **Sabina Bigi:** Writing – review & editing, Conceptualization. **Alessia Conti:** Writing – review & editing, Writing – original draft, Methodology, Investigation, Data curation. **Giovanni Gaglianone:** Methodology, Data curation. **Michela Ingrassia:** Writing – review & editing, Methodology, Data curation. **Francesco Latino Chiocci:** Writing – review & editing, Supervision. **Daniele Casalbore:** Writing – review & editing, Writing – original draft, Supervision, Investigation, Data curation, Conceptualization.

Declaration of competing interest

The authors declare that they have no known competing financial

interests or personal relationships that could have appeared to influence the work reported in this paper.

Data availability

Data will be made available on request.

Acknowledgments

The Authors wish to thank Guillem Mateus-Vicens and Nicoletta Mancin for their useful suggestions that greatly improved the manuscript. A special thank is for the BigBlueExplorers ASD, particularly the divers Claudio Provenzani and Andrea D'Ambrosi, for their precious support during the sampling surveys.

Appendix A. Supplementary data

Supplementary data to this article can be found online at <https://doi.org/10.1016/j.marpetgeo.2024.107130>.

References

- Alve, E., Goldstein, S.T., 2010. Dispersal, survival and delayed growth of benthic foraminiferal propagules. *J. Sea Res.* 63 (1), 36–51.
- Armynot du Châtelet, E.A., Gebhardt, K., Langer, M.R., 2011. Coastal pollution monitoring: foraminifera as tracers of environmental perturbation in the port of Boulogne-sur-Mer (Northern France). *Global Biogeochem. Cycles* 8 (4), 465–480. *N. Jb. Geol. Und Palaont. Abh.*, 262(1), 91. Bange, H.W., Bartell, U.H., Rapsomanikis, S., Andreae, M.O., 1994. Methane in the Baltic and North Seas and a reassessment of the marine emissions of methane.
- Bange, H.W., Bartell, U.H., Rapsomanikis, S., et al., 1994. Methane in the Baltic and North Seas and a reassessment of the marine emissions of methane. *Global Biogeochem Cycles* 8 (4), 465–480.
- Barletta, S., Del Bono, G.L., Salvati, L., 1969. Nota preliminare sui lavori geomorfologici e geominerari subacquei effettuati dal Servizio Geologico d'Italia dal 1964 al 1969. *Boll. Serv. Geol. It.* 83–89. CX.
- Baruffo, A., Ciaralli, L., Ardizzone, G., Gambi, M.C., Casoli, E., 2021. Ocean acidification and mollusc settlement in *Posidonia oceanica* meadows: does the seagrass buffer lower pH effects at CO₂ vents? *Diversity* 13, 311.
- Bergamin, L., Marassich, A., Provenzani, C., Romano, E., 2018. Foraminiferal ecozones in two submarine caves of the Orosei Gulf (Sardinia, Italy). *Rend. Lincei Scienze Fisiche e Naturali* 29 (3), 547–557.
- Bernhard, J.M., Goldstein, S.T., Bowser, S.S., 2010. An ectobiont-bearing foraminiferan, *Bolivina pacifica*, that inhabits microoxic pore waters: cell-biological and paleoceanographic insights. *Environ. Microbiol.* 12 (8), 2107–2119.
- Bernhard, J.M., Mollo-Christensen, E., Eisenkolb, N., Starczak, V.R., 2009. Tolerance of allogromiid Foraminifera to severely elevated carbon dioxide concentrations: implications to future ecosystem functioning and paleoceanographic interpretations. *Glob. Planet. Change* 65 (3–4), 107–114.
- Bernhard, J.M., 2000. Distinguishing live from dead foraminifera: methods review and proper applications. *Micropaleontology* 46, 38–46.
- Bernhard, J.M., Sen Gupta, B.K., 1999. Foraminifera of oxygen-depleted environments. In: *Modern Foraminifera*. Springer, Dordrecht. https://doi.org/10.1007/0-306-48104-9_12.
- Bernhard, J.M., Sen Gupta, B.K., Borne, P.F., 1997. Benthic foraminiferal proxy to estimate dysoxic bottom-water oxygen concentrations: santa Barbara Basin, U.S. Pacific continental margin. *J. Foraminif. Res.* 27, 301–310.
- Bernhard, J.M., 1988. Postmortem vital staining in benthic foraminifera: duration and importance in population and distributional studies. *J. Foraminif. Res.* 18, 143–146.
- Bouchet, V.M.P., Frontalini, F., Francescangeli, F., et al., 2021. Indicative value of benthic foraminifera for biomonitoring: assignment to ecological groups of sensitivity to total organic carbon of species from European intertidal areas and transitional waters. *Mar. Poll. Bull.* 164, 112071.
- Buosi, C., Châtelet, E.A.D., Cherchi, A., 2012. Benthic foraminiferal assemblages in the current-dominated strait of bonifacio (Mediterranean Sea). *Foraminif. Res.* 42 (1), 39–55.
- Capó-Bauçà, S., Whitney, S., Iniguez, C., et al., 2023. The trajectory in catalytic evolution of *Rubisco* in *Posidonia* seagrass species differs from terrestrial plants. *Plant Physiol* 191 (2), 946–956.
- Carminati, E., Doglioni, C., 2012. Alps vs. Apennines: the paradigm of a tectonically asymmetric Earth. *Earth Sci. Rev.* 112, 67–96. <https://doi.org/10.1016/j.earscirev.2012.02.004>.
- Casalbore, D., Ingrassia, M., Pierdomenico, et al., 2020. Morpho-acoustic characterization of a shallow-water mud volcano offshore Scoglio d'Affrica (Northern Tyrrhenian Sea) responsible for a violent gas outburst in 2017. *Mar. Geol.* 428, 106277. <https://doi.org/10.1016/j.margeo.2020.106277>.
- Cimerman, F., Langer, M.R., 1991. Mediterranean foraminifera. *Academia Scientiarum et Artium Slovenica: Ljubljana, Slovenia* 30, 1–11.
- Cinelli, F., Pardi, G., Papi, et al., 1993. I popolamenti bentonici delle isole dell'Arcipelago Toscano: Considerazioni ecologiche e Floristiche sul Phytobenthos ed elementi di Zoobenthos. Progetto mare ricerca sullo stato biologico chimico e fisico dell'Alto Mar Tirreno, pp. 313–394.
- Conrad, R., 2009. The global methane cycle: recent advances in understanding the microbial processes involved. *Environ. Microbiol. Rep.* 1 (5), 285–292.
- Cook, N.J., Ciobanu, C.L., Williams, T., 2011. The mineralogy and mineral chemistry of indium in sulphide deposits and implications for mineral processing. *Hydrometallurgy* 108 (3–4), 226–228.
- Cornamusini, G., Lazzarotto, A., Merlini, S., Pascucci, V., 2002. Eocene-miocene evolution of the north Tyrrhenian Sea. *Boll. Soc. Geol. It.* 1, 769–787. Volume Speciale n.
- Cornamusini, G., Pascucci, V., 2014. Sedimentation in the northern apennines–corsica tectonic knot (northern Tyrrhenian Sea, central mediterranean): offshore drilling data from the elba–pianosa ridge. *Int. J. Earth Sci.* 103, 821–842. <https://doi.org/10.1007/s00531-014-0998-5>.
- Damak, M., Fourati, R., Elleuch, B., Kallel, M., 2020. Environmental quality assessment of the fish farms' impact in the Monastir Bay (eastern of Tunisia, Central Mediterranean): a benthic foraminiferal perspective. *Environ. Sci. Pollut. Res.* 27, 9059–9074.
- Dando, P.R., Austen, M.C., Burke, Jr.R.A., et al., 1991. Ecology of a North Sea pockmark with an active methane seep. *Mar. Ecol. Prog. Ser.* 49–63.
- Dando, P.R., Hovland, M., 1992. Environmental effects of submarine seeping natural gas. *Contin. Shelf Res.* 12 (10), 1197–1207.
- De Nooijer, L.J., Toyofuku, T., Kitazato, H., 2009. Foraminifera promote calcification by elevating their intracellular pH. *Proc.Natl.Acad. Sci.* 106, 15374–15378.
- De Stigter, H.C., 1996. Recent and fossil benthic foraminifera in the Adriatic Sea: distribution patterns in relation to organic carbon flux and oxygen concentration at the seabed. *Geol. Ultraiect.* 144.
- Del Bono, G.L., Giammarino, S., 1968. Rinvenimento di manifestazioni metanifere nelle Praterie a Posidonia sui fondi marini prospicienti lo «Scoglio d'Affrica» nell'Arcipelago Toscano. *Atti Ist. Geol. Univ. Genova VI* (1), 11.
- Denman, S.E., Tomkins, N.W., McSweeney, C.S., 2007. Quantitation and diversity analysis of ruminal methanogenic populations in response to the antimethanogenic compound bromochloromethane. *FEMS Microbiol. Ecol.* 62 (3), 313–322.
- Dias, B.B., Hart, M.B., Smart, C.W., Hall-Spencer, J.M., 2010. Modern seawater acidification: the response of foraminifera to high-CO₂ conditions in the Mediterranean Sea. *J. Geol. Soc.* 167, 843–846.
- Di Bella, L., Conte, A.M., Conti, A., et al., 2022. Potential resilience to ocean acidification of benthic foraminifera living in *Posidonia oceanica* meadows: the case of the shallow venting site of Panarea. *Geosciences* 12, 184. <https://doi.org/10.3390/geosciences12050184>, 2022.
- Di Bella, L., Ingrassia, M., Frezza, V., et al., 2016. The response of benthic meiofauna to hydrothermal emissions in the Pontine Archipelago, Tyrrhenian Sea (central Mediterranean Basin). *J. Mar. Syst.* 164, 53–66, 2016.
- Figueira, B.O., Grenfell, H.R., Hayward, B.W., Alfaro, A.C., 2012. Comparison of Rose bengal and cell tracker green staining for identification of live salt-marsh foraminifera. *J. Foraminif. Res.* 42, 206–215.
- Folk, R.L., Ward, W.M., 1957. Brazos River bar: a study in the significance of grain size parameters. *J. Sediment. Petrol.* 27, 3–26.
- Fontaner, C., Jorissen, F.J., Licari, L., et al., 2002. Live benthic foraminiferal faunas from the Bay of Biscay: faunal density, composition, and microhabitats. *Deep Sea Res.* 1 49, 751–785.
- Fravega, P., Vannucci, G., 1982. Le Melobesie dei fondali dello «Scoglio d'Affrica» (Formiche di Montecristo). Forme ed associazioni in rapporto alle diverse situazioni ambientali. *Geol. Romana* 21, 687–692.
- Frontalini, F., Semprucci, F., Di Bella, L., et al., 2018. The response of cultured meiofaunal and benthic foraminiferal communities to lead exposure: results from mesocosm experiments. *Environ. Toxicol. Chem.* 37, 2439–2447.
- Geistdoerfer, P., Azuende, J.M., Batiza, et al., 1995. Hydrothermalisme et communautés animales associées sur la dorsale du pacifique oriental entre 17°S et 19°S (campagne Naudur, Decembre 1993). *Comptes Rendus de l'Académie des Sciences Serie II Mécanique, Physique, Chimie. Science de l'Univers* 320, 47–54.
- Glock, N., Schoenfeld, J., Mallon, J., 2012. In: Anoxia, Altenbach, A.V., Bernhard, J.M., Seckbach, J. (Eds.), *The Functionality of Pores in Benthic Foraminifera in View of Bottom Water Oxygenation; a Review*, pp. 539–552.
- Gupta, B.K.S., Machain-Castillo, M.L., 1993. Benthic foraminifera in oxygen-poor habitats. *Mar. Micropaleontol.* 20 (3–4), 183–201.
- Gupta, B.K.S., Platon, E., Bernard, J.M., Aharon, P., 1997. Foraminiferal colonization of hydrocarbon seep bacterial mats and underlying sediment, Gulf of Mexico slope. *J. Foramin. Res.* 27, 292–300.
- Hammer, Ø., Harper, D.A.T., 2006. *Paleontological Data Analysis*. Blackwell Publishing, Oxford.
- Hammer, Ø., Harper, D.A.T., Ryan, P.D., 2001. PAST: paleontological statistic software package for education and data analysis. *Palaentol. Electron.* 4, 9.
- Hannah, F., Rogerson, A., 1997. The temporal and spatial distribution of foraminifera in marine benthic sediments of the Clyde Sea, Scotland. *Estuar. Coast Shelf Sci.* 44, 377–383 [CrossRef].
- Hayward, B.W., Cedhagen, T., Kaminski, M., Gross, O., 2011. *World Modern Foraminifera Database*. Accessed through: <http://www.marinespecies.org/foraminifera/index.php>.
- Herguera, J.C., Paull, C.K., Perez, E., et al., 2014. Limits to the sensitivity of living benthic foraminifera to pore water carbon isotope anomalies in methane vent environments. *Paleoceanography* 29 (3), 273–289.

- Hill, T.M., Kennett, J.P., Valentine, D.L., 2004. Isotopic evidence for the incorporation of methane-derived carbon into foraminifera from modern methane seeps, Hydrate Ridge, Northeast Pacific. *Geochim. Cosmochim. Acta* 68 (22), 4619–4627.
- Hovland, M., Gardner, J.V., Judd, A.G., 2002. The significance of pockmarks to understanding fluid flow processes and geohazards. *Geofluids* 2 (2), 127–136. <https://doi.org/10.1046/j.1468-8123.2002.00028.x>.
- Ingrassia, M., Martorelli, E., Bosman, A., et al., 2015. The Zannone Giant Pockmark: first evidence of a giant complex seeping structure in shallow-water, central Mediterranean Sea, Italy. *Mar. Geol.* 363, 28–51.
- Jensen, P., Aagaard, L., Burke Jr, R.A., et al., 1992. “Bubbling reefs” in the Kattegat: submarine landscapes of carbonate-cemented rocks support a diverse ecosystem at methane seeps. *Mar. Ecol. Prog. Ser.* 83 (2/3), 103–112.
- Jerosch, K., Schlüter, M., Foucher, J.P., et al., 2007. Spatial distribution of mud flows, chemoautotrophic communities, and biogeochemical habitats at Håkon Mosby Mud Volcano. *Mar. Geol.* 243 (1–4), 1–17.
- Jorissen, F.J., Nardelli, M.P., Almogi-Labin, A., et al., 2018. Developing Foraminifera-AMBI for biomonitoring in the Mediterranean: species assignments to ecological categories. *Mar. Micropaleontol.* 140, 33–45. <https://doi.org/10.1016/j.marmicro.2017.12.006>.
- Judd, A., Hovland, M., 2009. *Seabed Fluid Flow: the Impact on Geology, Biology and the Marine Environment*. Cambridge University Press. <https://doi.org/10.1017/CBO9780511535918>.
- Kennett, J.P., Cannariato, K.G., Hendy, I.L., Behl, R.J., 2000. Carbon isotopic evidence for methane hydrate instability during quaternary interstadials. *Science* 288, 128–133.
- Knittel, K., Boetius, A., 2009. Anaerobic oxidation of methane: progress with an unknown process. *Annu. Rev. Microbiol.* 63, 311–334.
- Kopf, A.J., 2002. Significance of mud volcanism. *Rev. Geophys.* 40 (2), 1–2. <https://doi.org/10.1029/2000RG000093>.
- Kravchishina, M.D., Lein, A.Y., Flint, M.V., et al., 2021. Methane-Derived authigenic carbonates on the seafloor of the laptev sea shelf. *Front. Mar. Sci.* 8, 690304. <https://doi.org/10.3389/fmars.2021.690304>.
- Kuhnt, T., Schmiedl, G., Ehrmann, W., Hamann, Y., Hemleben, C., 2007. Deep-sea ecosystem variability of the aegean sea during the past 22 kyr as revealed by benthic foraminifera. *Mar. Micropaleontol.* 64 (3–4), 141–162.
- Langer, M.R., 1993. Epiphytic foraminifera. *Mar. Micropaleontol.* 20, 235–265.
- Langlet, D., Baal, C., Geslin, E., et al., 2014. Foraminiferal species responses to in situ, experimentally induced anoxia in the Adriatic Sea. *Biogeosciences* 11 (7), 1775–1797.
- Lei, Y.L., Li, T.G., Bi, H., et al., 2015. Responses of benthic foraminifera to the 2011 oil spill in the Bohai Sea, PR China. *Mar. Pollut. Bull.* 96, 245–260.
- Leutenegger, S., Hansen, H.J., 1979. Ultrastructural and radiotracer studies of pore function in Foraminifera. *Mar. Biol.* 54, 11.
- Levin, L.A., 2005. Ecology of cold seep sediments: interactions of fauna with flow, chemistry, and microbes. *Oceanogr. Mar. Biol., an Annual Review* 43, 1–46.
- Li, N., Feng, D., Wan, S., et al., 2021. Impact of methane seepage dynamics on the abundance of benthic foraminifera in gas hydrate bearing sediments: new insights from the South China Sea. *Ore Geol. Reviews* 136, 104247.
- Linke, P., Lutze, G.F., 1993. Microhabitat preferences of benthic foraminifera—a static concept or a dynamic adaptation to optimize food acquisition? *Mar. Micropaleontol.* 20, 215–234.
- Loeblich, R., Tappan, H., 1987. *Foraminiferal Genera and Their Classification*. Van Nostrand Reinhold, New York.
- Luth, C., Luth, U., Gebruk, A.V., Thiel, H., 1999. Methane gas seeps along the oxic/anoxic gradient in the Black Sea: manifestations, biogenic sediment compounds and preliminary results on benthic ecology. *Mar. Ecol.* 20 (3–4), 221–249.
- Lutze, G.F., Altenbach, A., 1991. Technik und Signifikanz der Lebendfärbung benthischer Foraminiferen mit Begalrot. *Geol. Jahrb.* 128, 251–265.
- Mackensen, A., Wollenburg, J., Licari, L., 2006. Low $\delta^{13}\text{C}$ in tests of live epibenthic and endobenthic foraminifera at a site of active methane seepage. *Paleoceanography* 21 (2).
- Magno, M.C., Bergamin, L., Foinia, M.G., et al., 2012. Correlation between textural characteristics of marine sediments and benthic foraminifera in highly anthropogenically-altered coastal areas. *Mar. Geol.* 315, 143–161.
- Mateu-Vicens, G., Khokhlova, A., Sebastián-Pastor, T., 2014. Epiphytic foraminiferal indices as bioindicators in Mediterranean seagrass meadows. *J. Foramin. Res.* 44 (3), 325–339.
- Mazzini, A., Etiope, G., 2017. Mud volcanism: an updated review. *Earth Sci. Rev.* 168, 81–112. <https://doi.org/10.1016/j.earscirev.2017.03.001>.
- McCorkle, D.C., Corliss, B.H., Farnham, C., 1997. Vertical distributions and isotopic compositions of live (stained) benthic foraminifera from the North Carolina and California continental margins. *Deep-Sea Res.* 44, 983–1024.
- McCorkle, D.C., Keigwin, L.D., Corliss, B.H., Emerson, S.R., 1990. The influence of microhabitats on the carbon isotopic composition of deep-sea benthic foraminifera. *Paleoceanography* 5, 161–185.
- Meister, P., Wiedling, J., Lott, C., et al., 2018. Anaerobic methane oxidation inducing carbonate precipitation at abiogenic methane seeps in the Tuscan archipelago (Italy). *PLoS One* 13 (12), e0207305.
- Mendes, I., Dias, J.A., Schönfeld, J., Ferreira, Ó., 2012. Distribution of living benthic foraminifera on the northern Gulf of Cadiz continental shelf. *J. Foramin. Res.* 42 (1), 18–38.
- Motteran, G., Ventura, G., 2005. Aspetti geologici, morfologici e ambientali dello Scoglio d’Africa (Arcipelago Toscano): Nota preliminare. *Atti Della Società Toscana di Scienze Naturali. Memorie Serie A* 110, 51–60.
- Murray, J.W., 1991. *Ecology and Palaeoecology of Benthic Foraminifera*, first ed. Routledge. <https://doi.org/10.4324/9781315846101>.
- Murray, J.W., 2006. *Ecology and Applications of Benthic Foraminifera*. Cambridge University Press, Cambridge.
- Murray, J.W., Bowser, S.S., 2000. Mortality, protoplasm decay rate, and reliability of staining techniques to recognize ‘living’ foraminifera: a review. *J. Foraminif. Res.* 30, 66–77.
- Panieri, G., 2003. Benthic foraminifera response to methane release in an Adriatic Sea pockmark. *Riv. It. Paleontol. Strat.* 109 (3), 549–562.
- Panieri, G., 2006. Foraminiferal response to an active methane seep environment: a case study from the Adriatic Sea. *Mar. Micropaleontol.* 61 (1–3), 116–130.
- Panieri, G., Graves, C.A., James, R.H., 2016. Paleomethane emissions recorded in foraminifera near the landward limit of the gas hydrate stability zone offshore western Svalbard. *Geochim., Geophys., Geosyst.* 17 (2), 521–537.
- Panieri, G., James, R.H., Camerlenghi, A., et al., 2014. Record of methane emissions from the West Svalbard continental margin during the last 23,500 yrs revealed by $\delta^{13}\text{C}$ of benthic foraminifera. *Glob. Planet. Change* 122, 151–160.
- Panieri, G., Gamberi, F., Marani, M., Barbieri, R., 2005. Benthic foraminifera from a recent, shallow-water hydrothermal environment in the Aeolian Arc (Tyrrhenian Sea). *Mar. Geol.* 218, 207–229.
- Pettit, L.R., Hart, M.B., Medina-Sánchez, A.N., et al., 2013. Benthic foraminifera show some resilience to ocean acidification in the northern Gulf of California, Mexico. *Mar. Pollut. Bull.* 73, 452–462.
- Pletnev, S.P., Annin, V.K., Vu, Yu, et al., 2014. Foraminifera and isotopes $\text{O}^{16}/\text{O}^{18}$ and $\text{C}^{12}/\text{C}^{13}$ of their tests in methane outlets on the eastern slope of Sakhalin peninsula, Sea of Okhotsk. *Izvestiya TINRO* 178, 180–190.
- Polikarpov, G.G., Tereschenko, N.N., Gulín, M.B., 1998. Chemoecological study of the bivalve *Modiolus phaseolinus* in habitats near the oxic/anoxic interface near methane gas seeps in the Black Sea. In: Luth, U., Luth, C., Thiel, H. (Eds.), *MEGASEEBS-methane Gas Seeps Exploration in the Black Sea*, Berichte aus dem Zentrum für Meeres und Klimaforschung, vol. 14, pp. 92–100.
- Portnova, D.A., Mokievskiy, V.O., Khaflidason, Kh, et al., 2014. Multicellular meiofauna and taxocene of nematodes in the area of methane outlets of Niega (Norwegian Sea). *Biol. Morya* 40 (4), 268–278 (in Russian).
- Ramajo, L., Lagos, N.A., Duarte, C.M., 2019. Seagrass *Posidonia oceanica* diel pH fluctuations reduce the mortality of epiphytic forams under experimental ocean acidification. *Mar. Pollut. Bull.* 146, 247–254.
- Ramaswamy, V., Chanin, M.L., Angell, J., et al., 2001. Stratospheric temperature trends: observations and model simulations. *Rev. Geophys.* 39 (1), 71–122.
- Rathburn, A.E., Levin, L.A., Held, Z., Lohmann, K.C., 2000. Benthic foraminifera associated with cold methane seeps on the northern California margin: ecology and stable isotopic composition. *Mar. Micropaleontol.* 38 (3–4), 247–266.
- Rathburn, A.E., Pérez, M.E., Martin, J.B., et al., 2003. Relationships between the distribution and stable isotopic composition of living benthic foraminifera and cold methane seep biogeochemistry in Monterey Bay, California. *Geochim. Geophys. Geosyst.* 4 (12).
- Rathburn, A.E., Corliss, B.H., Tappa, K.D., Lohmann, K.C., 1996. Comparisons of the ecology and stable isotopic compositions of living (stained) deep-sea benthic foraminifera from the Sulu and South China Seas. *Deep-Sea Res.* 43, 1617–1646.
- Rathburn, A.E., Willingham, J., Ziebis, W., et al., 2018. A new biological proxy for deep-sea paleo-oxygen: Pores of epifaunal benthic foraminifera. *Scientific Report* 8 (1), 9456.
- Rhee, T.S., Kettle, A.J., Andreae, M.O., 2009. Methane and nitrous oxide emissions from the ocean: a reassessment using basin-wide observations in the Atlantic. *J. Geophys. Res.: Atmospheres* 114 (D12).
- Romano, E., Bergamin, L., Ausili, A., et al., 2009. The impact of the Bagnoli industrial site (Naples, Italy) on sea-bottom environment. Chemical and textural features of sediments and the related response of benthic foraminifera. *Mar. Poll. Bull.* 59 (8–12), 245–256.
- Romano, E., Bergamin, L., Di Bella, L., et al., 2021. Benthic foraminifera as environmental indicators in extreme environments: the marine cave of Bue Marino (Sardinia, Italy). *Ecol. Indic.* 120, 106977.
- Rosentreter, J.A., Borges, A.V., Deemer, B.R., et al., 2021. Half of global methane emissions come from highly variable aquatic ecosystem sources. *Nat. Geosci.* 14 (4), 225–230.
- Ruff, S.E., Kuhfuss, H., Wegener, G., et al., 2016. Methane seep in shallow-water permeable sediment harbors high diversity of anaerobic methanotrophic communities, Elba, Italy. *Front. Microbiol.* 7 (374).
- Saroni, A., Sciarra, A., Grassa, F., et al., 2020. Shallow submarine mud volcano in the northern Tyrrhenian sea, Italy. *Appl. Geochem.* 122, 104722. <https://doi.org/10.1016/j.apgeochem.2020.104722>.
- Schmiedl, G., Mitschele, A., Beck, S., et al., 2003. Benthic foraminiferal record of ecosystem variability in the eastern Mediterranean Sea during times of sapropel S5 and S6 deposition. *Palaeogeog. Palaeoclimatol. Palaeoecol.* 190, 139–164.
- Schönfeld, J., 2002. Recent benthic foraminiferal assemblages in deep high-energy environments from the Gulf of Cadiz (Spain). *Mar. Micropaleontol.* 44, 141–162.
- Schönfeld, J., 1997. The impact of the Mediterranean Outflow Water (MOW) on benthic foraminiferal assemblages and surface sediments at the southern Portuguese continental margin. *Mar. Micropaleontol.* 29, 211–236.
- Schönfeld, J., Alve, E., Geslin, E., et al., 2012. The Fobimo (Foraminiferal Bio-Monitoring) initiative—towards a standardized protocol for soft-bottom benthic foraminiferal monitoring studies. *Mar. Micropaleontol.* 94–95, 1–13.
- Schorn, S., Ahmerkamp, S., Bullock, E., et al., 2022. Diverse methylophilic methanogenic archaea cause high methane emissions from seagrass meadows. *Proc. Nati. Acad. Sci.* 119 (9), e2106628119.
- Schott, W., 1935. Die foraminiferen in den Äquatorialen teil des atlantischen ozeans. *Deutsche Atlantische Expedition* 6, 411–616.

- Schwing, P.T., Romero, I.C., Brooks, G.R., et al., 2015. A decline in benthic foraminifera following the deepwater horizon event in the Northeastern Gulf of Mexico. *PLoS One* 10 (5), e0128505.
- Scott, D.B., Medioli, F.S., Schafer, C.T., 2001. *Monitoring of Coastal Environments Using Foraminifera and Thecamoebian Indicators*. Cambridge University Press, Cambridge, UK.
- Sgarrella, F., Montcharmont-Zei, M., 1993. Benthic foraminifera of the Gulf of Naples (Italy): systematics and autoecology. *Boll. Soc. Paleontol. It.* 32, 145–264.
- Shank, T.M., Fornari, D.J., Von Damm, K.L., et al., 1998. Temporal and spatial patterns of biological community development at nascent deep-sea hydrothermal vents (9°50' N, East Pacific Rise). *Deep Sea Res. Part II Top. Stud. Oceanogr.* 45 (1–3), 465–515.
- Shannon, C.E., 1948. A mathematical theory of communication. *Bell Syst. Tech. J.* 27, 379–423.
- Shnyukov, E., Yanko-Hombach, V., 2020. *Mud Volcanoes of the Black Sea Region and Their Environmental Significance*. Springer, Switzerland, pp. 1–491.
- Spatola, D., Casalbore, D., Pierdomenico, M., et al., 2023. Seafloor characterization of the offshore sector around Scoglio d'Affrica islet (Tuscan Archipelago, northern Tyrrhenian sea). *J. Maps*. <https://doi.org/10.1080/17445647.2022.2120836>.
- Sreenivasulu, G., Praseetha, B.S., Daud, N.R., et al., 2019. Benthic foraminifera as potential ecological proxies for environmental monitoring in coastal regions: a study on the Beypore estuary, Southwest coast of India. *Mar. Poll. Bull.* 138, 341–351.
- Thomas, E., 2003. Extinction and food at the seafloor: a high-resolution benthic foraminiferal record across the initial Eocene thermal maximum, southern ocean site 690. *Special Papers-Geol. Soc. Am. Spec. Pap.* 319–332.
- Vizzini, S., Tomasello, A., Maida, G.D., et al., 2010. Effect of explosive shallow hydrothermal vents on $\delta^{13}\text{C}$ and growth performance in the seagrass *Posidonia oceanica*. *J. Ecol.* 98 (6), 1284–1291.
- Walton, W., 1952. Techniques for recognition of living foraminifera, Cushman Found. *Foram. Res.* 3, 56–60.
- Wiedicke, M., Weiss, W., 2006. Stable carbon isotope records of carbonates tracing fossil seep activity off Indonesia. *Geochem. Geophys. Geosyst.* 7 (11).
- Yanko, V., Arnold, A., Parker, W., 1999. The effect of marine pollution on benthic Foraminifera. In: Sen Gupta, B.K. (Ed.), *Modern Foraminifera*. Kluwer Academic Publishers, Dordrecht, pp. 217–238.
- Yanko, V.V., Kadurin, V.M., Kravchuk, A., et al., 2023. Influence of methane and other hydrocarbon gases on foraminifera and nematodes in the Northwestern part of the Black Sea. *Mar. Environ. Res.* 193, 106285.
- Yanko, V.V., Kadurin, V.M., Chepizhko, O.V., et al., 2017. Development of Forecast Criteria in the Search of Investigations in the Black Sea Based the Theory of Fluidogenesis, pp. 1–181. Report on Scientific Research Work. State Registration Number 0119U002196.